Experimental Neurology 330 (2020) 113355

Contents lists available at ScienceDirect

Experimental Neurology

journal homepage: www.elsevier.com/locate/yexnr

Research paper

Regeneration of adult rat sensory and motor neuron axons through chimeric peroneal nerve grafts containing donor Schwann cells engineered to express different neurotrophic factors

Maria João Godinho[a], Jonas L. Staal[a], Vidya S. Krishnan[a], Stuart I. Hodgetts[a,b], Margaret A. Pollett[a], Douglas P. Goodman[c], Lip Teh[d], Joost Verhaagen[e], Giles W. Plant[f], Alan R. Harvey[a,b,*]

[a] School of Human Sciences, The University of Western Australia, Crawley, WA 6009, Australia
[b] Perron Institute for Neurological and Translational Science, Nedlands, WA 6009, Australia
[c] School of Veterinary and Biomedical Sciences, Murdoch University, Murdoch, WA 6150, Australia
[d] Plastic Surgery Centre, St John of God Hospital, Murdoch, WA 6150, Australia
[e] Netherlands Institute for Neuroscience, Meibergdreef 47, Amsterdam, the Netherlands
[f] Department of Neurosurgery, Stanford University School of Medicine, Stanford, CA 94305, USA

ARTICLE INFO

Keywords:
Peripheral nerve repair
Neurotrophins
Gene therapy
Schwann cell transplantation
Dorsal root ganglia
Motor neurons

ABSTRACT

Large peripheral nerve (PN) defects require bridging substrates to restore tissue continuity and permit the regrowth of sensory and motor axons. We previously showed that cell-free PN segments repopulated *ex vivo* with Schwann cells (SCs) transduced with lentiviral vectors (LV) to express different growth factors (BDNF, CNTF or NT-3) supported the regeneration of axons across a 1 cm peroneal nerve defect (Godinho et al., 2013). Graft morphology, the number of regrown axons, the ratio of myelinated to unmyelinated axons, and hindlimb locomotor function differed depending on the growth factor engineered into SCs. Here we extend these observations, adding more LVs (expressing GDNF or NGF) and characterising regenerating sensory and motor neurons after injection of the retrograde tracer Fluorogold (FG) into peroneal nerve distal to grafts, 10 weeks after surgery. Counts were also made in rats with intact nerves and in animals receiving autografts, acellular grafts, or grafts containing LV-GFP transduced SCs. Counts and analysis of FG positive ($^+$) DRG neurons were made from lumbar (L5) ganglia. Graft groups contained fewer labeled sensory neurons than non-operated controls, but this decrease was only significant in the LV-GDNF group. These grafts had a complex fascicular morphology that may have resulted in axon trapping. The proportion of FG$^+$ sensory neurons immunopositive for calcitonin-gene related peptide (CGRP) varied between groups, there being a significantly higher percentage in autografts and most neurotrophic factor groups compared to the LV-CNTF, LV-GFP and acellular groups. Furthermore, the proportion of regenerating isolectin $B_4$$^+$ neurons was significantly greater in the LV-NT-3 group compared to other groups, including autografts and non-lesion controls. Immunohistochemical analysis of longitudinal graft sections revealed that all grafts contained a reduced number of choline acetyltransferase (ChAT) positive axons, but this decrease was significant only in the GDNF and NT-3 graft groups. We also assessed the number and phenotype of regrowing lumbar FG$^+$ motor neurons in non-lesioned animals, and in rats with autografts, acellular grafts, or in grafts containing SCs expressing GFP, CNTF, NGF or NT-3. The overall number of FG$^+$ motor neurons per section was similar in all groups; however in tissue immunostained for NeuN (expressed in α- but not γ-motor neurons) the proportion of NeuN negative FG$^+$ neurons ranged from about 40–50% in all groups except the NT-3 group, where the percentage was 82%, significantly more than the SC-GFP group. Immunostaining for the vesicular glutamate transporter VGLUT-1 revealed occasional proprioceptive terminals in 'contact' with regenerating FG$^+$ α-motor neurons in PN grafted animals, the acellular group having the lowest counts. In sum, while all graft types supported sensory and motor axon regrowth, there appeared to be

Abbreviations: BDNF, Brain-derived neurotrophic factor; CGRP, Calcitonin-gene related peptide; ChAT, Choline acetyltransferase; CNTF, Ciliary neurotrophic factor; DRG, Dorsal root ganglion; FG, FluoroGold; GDNF, Glial cell-derived neurotrophic factor; GFP, Green fluorescent protein; IB_4, Isolectin B_4; LV, Lentiviral vectors; NeuN, Neuronal DNA binding protein; NGF, Nerve growth factor; NT-3, Neurotrophin-3; PN, Peripheral nerve; SC, Schwann cells; VGLUT-1, Vesicular glutamate transporter-1

* Corresponding author at: School of Human Sciences M309, The University of Western Australia, 35 Stirling Highway, Crawley, WA 6009, Australia.
E-mail address: alan.harvey@uwa.edu.au (A.R. Harvey).

https://doi.org/10.1016/j.expneurol.2020.113355
Received 26 February 2020; Received in revised form 28 April 2020; Accepted 4 May 2020
Available online 15 May 2020
0014-4886/

axon trapping in SC-GDNF grafts, and data from the SC-NT-3 group revealed greater regeneration of sensory $CGRP^+$ and IB_4^+ neurons, preferential regeneration of γ-motor neurons and perhaps partial restoration of monosynaptic sensorimotor relays.

1. Introduction

After a peripheral nerve (PN) injury, affected neurons must first survive the initial trauma if they are to regrow their axons and re-establish connections with peripheral targets. Extensive PN injury involving more than a critical length of damaged tissue requires the use of bridging substrates such as PN grafts to re-establish continuity between proximal and distal stumps. Subsequent examination of such grafts and host nerve stumps can provide data on the number and distribution of regenerating axons but does not directly give information about neuronal survival and the source of the regenerating axons. The number of axons in grafts may include multiple sprouts from a single axon as well as axons that have turned around and are now travelling back along the nerve.

Using an alternative to autologous nerve grafts, we previously showed that allogeneic acellular PN sheaths repopulated *ex vivo* with congeneic Schwann cells (SCs) transduced with lentiviral vectors (LV) to express different growth factors (either brain-derived neurotrophic factor - BDNF, ciliary neurotrophic factor - CNTF or neurotrophin-3 – NT-3) supported the regeneration of many axons across a 1 cm peroneal nerve defect (Godinho et al., 2013). The morphology of these grafts, the number and type of regenerating axons, the ratio of myelinated to unmyelinated axons, myelin thickness and hindlimb locomotor function all varied depending on the growth factor that had been engineered into the transplanted SCs. In the present study, using the same chimeric graft model, our aim was to quantify neuronal survival after injury and characterize the sensory and motor neurons that regrew axons through and beyond the different graft types. To do this, the retrograde tracer FluoroGold (FG) was injected into peroneal nerve distal to the grafts, 10 weeks after surgery. In addition to the genetically modified SCs described above, in the present study we also grafted PN repopulated with SCs transduced with LV encoding either glial cell-derived neurotrophic factor (GDNF) or nerve growth factor (NGF). Counts were also made in normal animals with intact nerves, and in rats receiving autografts, acellular grafts, or grafts containing 'control' SCs engineered to express only green fluorescent protein (GFP).

The peroneal nerve is a mixed nerve containing both afferent and efferent axons; thus we counted and analyzed FG positive ($^+$) neurons in lumbar dorsal root ganglia (DRG) known to contribute sensory axons to the rat peroneal nerve (Swett et al., 1991), and examined FG^+ motor neurons in relevant segments of ventral horn of the spinal cord. In addition to determining the number of regenerating sensory and motor neurons for each graft type, FG identification was combined with immunofluorescence labelling with several antibodies to permit some phenotypic characterization of the regenerating neuronal populations. For DRG neurons, the panel of antibodies included the neuronal markers isolectin B_4 (IB_4) and calcitonin gene-related peptide (CGRP), and antibodies against various neurotrophic factor receptors. In transverse lumbar spinal cord sections, neuronal DNA binding protein (NeuN) antibodies were used to distinguish between alpha (α) and gamma (γ) motor neurons, the latter reported to express low levels of this protein (Friese et al., 2009). An additional series of spinal cord sections containing FG^+ neurons was immunostained with antibodies to βIII-tubulin and the vesicular glutamate transporter-1 (VGLUT-1), the latter a marker for the terminals of primary 1a afferents originating from muscle spindles (Todd et al., 2003; Alvarez et al., 2011; Levine et al., 2014; Liu et al., 2014). This was done in order to determine if sensory feedback was restored to regenerate motor neurons (Mendell et al., 1999). Finally, longitudinal sections of graft tissue were immunostained with an antibody to central choline acetyl transferase (ChAT) to assess the regeneration of cholinergic motor neurons and their axons within the genetically modified grafts.

2. Materials and methods

2.1. Experimental animal groups and surgical procedures

Fischer 344 rats were obtained from the Animal Resource Centre (Western Australia) and housed under standard conditions with a 12 h light/dark cycle and *ad libitum* access to food and water. Surgical

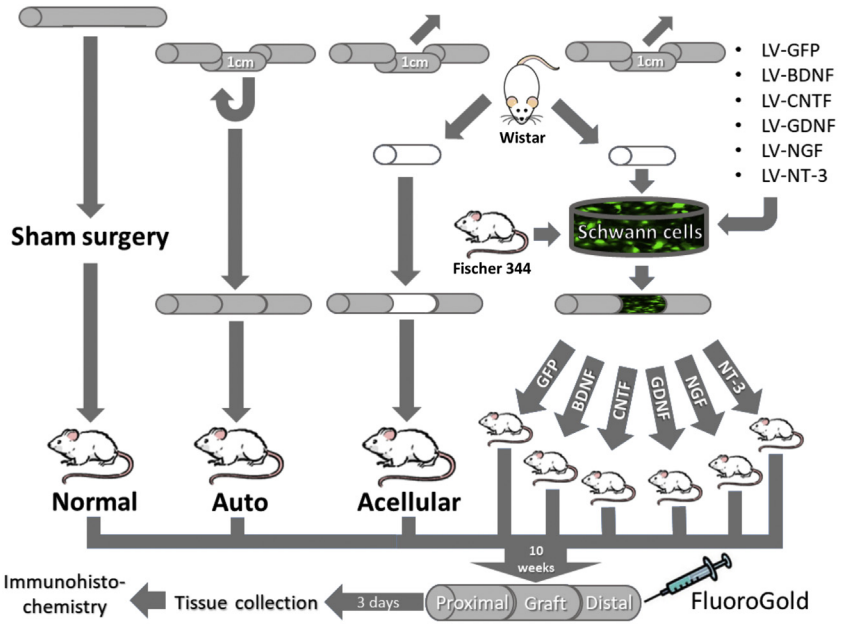

Fig. 1. Summary of experimental protocols and groups. Freeze-thawed segments of Wistar peroneal nerve repopulated *ex vivo* with genetically modified Schwann cells were grafted into 1 cm peroneal nerve defects in Fischer 344 rats. After 10 weeks, FluoroGold was injected into host nerve distal to the grafts to analyze regeneration of sensory and motor neurons.

procedures followed Australia's NHMRC guidelines and were approved by the UWA's Animal Ethics Committee. There were 9 experimental groups, each containing 5 adult (8–10 week old) male Fischer rats. Normal (control) rats were uninjured, while in all other animals the peroneal nerve on the left hindlimb was transected and grafted with different types of PN tissue: autografts (in which 1 cm segment of the nerve was completely sectioned and sutured back into the nerve defect), acellular PN sheaths, or allogeneic PN sheaths that had been re-populated *ex vivo* with Fischer-derived SCs genetically modified using LV vectors to express different growth factors or control SCs genetically modified to express the reporter gene GFP (Fig. 1). Rats were anaesthetized with an intra-peritoneal injection (1 ml/kg body weight) of a mixture of equal volume of ketamine (100 mg/ml) and xylazine (20 mg/ml), the peroneal nerve exposed and a 1 cm segment removed. The nerve gap was immediately repaired with a graft attached to proximal and distal nerve stumps using 10/0 nylon suture (Ethilon). Skin was closed with 6/0 suture (Ethilon) and animals were given Benacillin ((200 µl/100 g of body weight, 64 mg/kg, 300 U/ml) intramuscularly and Temgesic (20 µg/kg body weight, 0.0324 mg/kg, 300 U/ml) subcutaneously.

2.2. Preparation of acellular nerve sheaths

Acellular sheaths are non-immunogenic PN segments that have been freeze-thawed to kill endogenous cells while maintaining the integrity of the basal lamina (Gulati, 1995; Cui et al., 2003). As described previously (Godinho et al., 2013) acellular sheaths were prepared from peroneal nerves of allogeneic (Wistar) adult male rats and inserted into similar nerves in F344 host rats. Cells were removed by 5 consecutive cycles of 5 min freezing in liquid nitrogen and 5 min thawing at room temperature, followed by storage at −80 °C. One experimental group received acellular nerve sheaths prepared as described and trimmed to 1 cm (acellular group), while others received nerve sheaths which were seeded with genetically modified SCs prior to grafting.

2.3. Preparation and genetic modification of adult SC cultures using lentiviral vectors (LV)

The methods used to obtain primary cultures of adult SCs and their subsequent transduction have been described (Morrissey et al., 1991; Plant et al., 2002; Cui et al., 2003; Hu et al., 2005, 2007; Godinho et al., 2013). Briefly, to prepare each culture, five F344 rats were sacrificed and their sciatic nerves collected, placed in Liebovitz's L-15 medium (Invitrogen), stripped of their epineurium and sectioned into 1-2 mm pieces. Explants were incubated at 37 °C with 5% CO_2 in D10 media (Dulbecco's Modified Eagle's Medium (DMEM)) (Sigma) with 10% foetal bovine serum (FBS) (Sigma), 1% L-glutamine (Invitrogen) and 1% penicillin/streptomycin (Invitrogen). Every week for about a month explants were transferred into clean dishes to discard plated fibroblasts which are quicker than SCs in migrating out of the nerve pieces. Explants were then enzymatically dissociated overnight with 1.25 U/ml dispase (Boehringer Mannheim Biochemicals) and 0.05% collagenase (Sigma) in DMEM with 15% FBS. The resulting SC cultures were expanded on poly-L-lysine (Sigma) coated dishes containing D10 media with 20 µg/ml bovine pituitary extract (GibcoBRL) and 2 µM forskolin (Sigma).

For the transduction, approximately 10^6 SCs were plated for 24 h and incubated with each of the LV stocks (titers between 10^8 and 10^9 transducing units/ml; MOI of 50) for 24 h. As described previously (Godinho et al., 2013), cultures were incubated in fresh D10 for further 48 h to allow maximal transgene expression. The LV stocks used encoded either: green fluorescent protein (GFP), brain derived neurotrophic factor (BDNF), ciliary neurotrophic factor (CNTF), glial cell-derived neurotrophic factor (GDNF), nerve growth factor (NGF) or neurotrophin-3 (NT-3). These LV vectors were similar to those described and carefully characterized *in vitro* and *in vivo* elsewhere (Hu

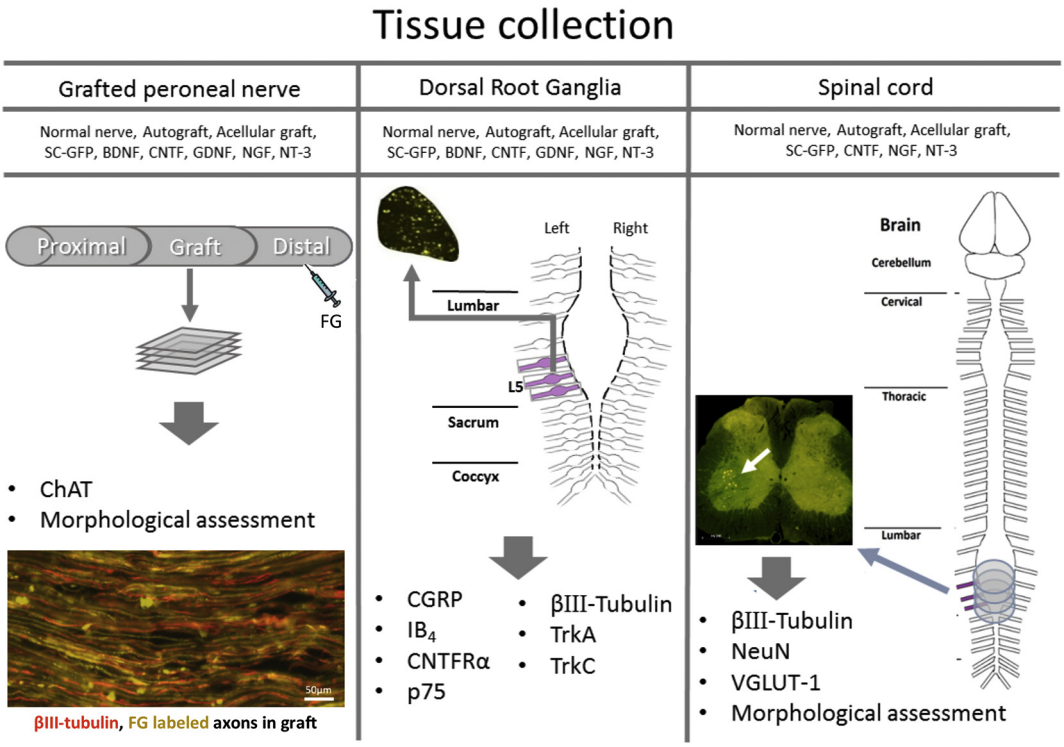

Fig. 2. Summary of tissue collection and immunohistochemical analysis using the listed antibodies. Peroneal nerve grafts were sectioned longitudinally; the image bottom left shows a section containing retrogradely labeled FluoroGold (FG) positive axons that are immunopositive for βIII-tubulin (red), scale bar = 50 µm. Counts of regenerate FG labeled neurons were made in sections of L5 dorsal root ganglia and transverse sections of lumbar spinal cord (arrow). (For interpretation of the references to colour in this figure legend, the reader is referred to the web version of this article.)

et al., 2005, 2007; Eggers et al., 2008; Hoyng et al., 2014).

2.4. Seeding of freeze-thawed peroneal nerve sheaths with genetically modified SCs

We previously described the seeding of acellular sheaths with SCs (Cui et al., 2003; Hu et al., 2005; Godinho et al., 2013). Briefly, cultured SCs were rinsed twice with Ca^{2+} and Mg^{2+} free Hanks balanced salt solution (Sigma), incubated with 0.05% trypsin (CSL) and 0.02% EDTA (Invitrogen) for 5 min at 37 °C, rinsed with D10, centrifuged at 10^3 rpm and resuspended to 5×10^4/μl in D10. Acellular nerve sheaths incubating in D10 were trimmed to 1 cm length and, using a glass micropipette in a Hamilton syringe, 1 μl of SC suspension was slowly injected into both ends of the nerve, aiming for the optimal concentration of 10^5 SCs/sheath. Exactly the same injection technique was used for all reconsituted graft types. Sheaths were then incubated for 24 h in a drop of SC suspension to promote further infiltration. Subsequently these repopulated sheaths were used to repair 1 cm gaps in left hindlimb peroneal nerve of F344 host rats in the experimental groups SC-GFP, BDNF, CNTF, GDNF, NGF and NT-3 (see above 'surgical procedures' section).

2.5. Retrograde labelling of cell bodies

Ten weeks after PN graft surgery, rats were anaesthetized as described previously, their grafted peroneal nerve exposed and 0.2 μl of 4% FluoroGold (FG) (Fluorochrome Inc.) slowly injected *via* a pulled glass pipette attached to a 10 μl Hamilton syringe into the host nerve stump several mm distal to the graft (Fig. 1). Great care was taken to ensure FG did not leak into the distal end of each graft. The uninjured group of animals received a FG injection into their intact left hindlimb peroneal nerve to determine baseline numbers and normal distribution of neurons in dorsal root ganglia and ventral horn of the spinal cord. Animals received post-operative care and survived for 3 days to allow retrograde transport of the tracer.

2.6. Tissue collection and processing

Rats were deeply anaesthetized with an intra-peritoneal injection of sodium pentobarbitone (Lethabarb, 325 mg/kg) and perfused transcardially with heparinized phosphate buffered saline (PBS, 0.1 M pH 7.4) and then 4% paraformaldehyde in the same buffer. Collections from every animal included the left peroneal nerve – containing the grafted tissue, the fourth to sixth lumbar DRGs, and in 7 of the 9 groups the lumbosacral regions of the spinal cord to analyze motor neuron regeneration (Fig. 2). Due to problems during tissue processing, appropriate regions of the lumbar spinal cord from the LV-BDNF and LV-GDNF groups could not be analyzed. Fixed nerves were gently straightened onto a wooden spatula and cryoprotected in 30% sucrose solution for 24 h at 4 °C. PNs, DRGs and dissected spinal cords were embedded in OCT (tissue freezing medium, Leica), snap frozen in isopentane (2-methylbutane) and stored at −80 °C. Using a Leica CM3050 cryostat 16 μm thick longitudinal sections of the peroneal nerve with graft were collected in a series of 5 gelatine coated slides. DRGs were cut into 20 μm thick sections assembled in series of 5 slides, air-dried and stored at −20 °C. Spinal cords were thawed and gently rinsed in PBS. The cords were cut into three blocks and each block was embedded in 10% gelatine PBS, aligned from rostral to caudal. Tissue was cryoprotected in 30% sucrose in PBS overnight at 4 °C and stored in −20 °C freezer until sectioning. Gelatine fixed spinal cords were mounted and covered with fresh OCT and cut into 40 μm thick sections in a Leica CM3050 cryostat at −20 °C. Cut sections were placed free floating in 0.02% sodium azide in PBS. Series of sections were put in pairs in 24-well plates.

2.7. Immunofluorescence staining

Immunostaining protocols and selected antibodies differed slightly, depending on whether DRG, nerves or spinal cords were being processed (Fig. 2). From storage, DRG slides were dried at room temperature in a humidified dark chamber with gentle agitation. Sections were rinsed 3× with PBS for 5 min, blocked for 1 h in primary antibody diluent (PBS with 10% normal horse serum and 0.2% Triton X-100, and incubated overnight in diluent with primary antibodies at 4 °C. Immunostaining runs included a negative control with no primary antibody. DRG sections were immunostained stained with IB_4 (Invitrogen #18-0171Z (Zymed), 1:500) to identify primary nonpeptidergic sensory neurons, CGRP (AbD Serotec #1720–9007, 1:400) for primary peptidergic sensory neurons, or antibodies against neurotrophic factor receptors, namely, the tropomyosin receptor kinases (Trk) A (Millipore #AB1577, 1:500) and TrkC (Biosensis #R-151–100, 1:500), receptor p75 (Promega #G323A, 1:1000) and ciliary neurotrophic receptor alpha (CNTFRα) (AbD Serotec #1720–9007, 1:1000). Secondary antibodies used for DRG staining were either goat anti-rabbit Cy3 (Jackson ImmunoResearch Labs #111–166-006, 1:300), donkey anti-goat Cy3 (Jackson ImmunoResearch Labs #705–166-147, 1:1000), donkey anti-goat Alexa Fluor 488 (Invitrogen #A11055, 1:1000), or goat anti-rabbit FITC (Sigma #F6005, 1:100). Sections were washed 3× with PBS for 5 min, appropriate secondary antibody dilutions were added for 1 h, and sections were washed as described. Slides were covered with fluorescence mounting medium (DAKO), cover-slipped and kept in the dark at 4 °C.

Longitudinal PN sections were stained using protocols similar to the above with neurofilament (PanNF) (Invitrogen #18-0171Z, 1:500) for axonal neurofilaments or βIII-tubulin (TuJ1, Covance #MMS-435P, 1:400 for axonal microtubules, and goat anti-mouse Cy3 (Jackson ImmunoResearch Labs #115–166-006, 1:500) as the secondary antibody. For ChAT immunostaining, an additional step of antigen retrieval was added in the beginning, which involved a 10 min wash with 0.1% Triton-X100 and 10 μg/ml proteinase k in PBS and overnight incubation at 55 °C in 50% formamide. This procedure enhances antibody penetration and optimizes visualization of ChAT (Eggers et al., 2010; Shakhbazau et al., 2012). This was followed by routine immunohistochemical protocol using an antibody to central ChAT (Chemicon #AB144P, 1:1000), followed by donkey anti-goat Alexa Fluor 488 (1:1000).

Free-floating spinal cord sections were rinsed in PBS, then blocked for 30 min on a shaker tray in antibody diluent (PBS with 10% normal goat serum and 0.2% Triton X-100). Sections were incubated overnight in primary antibody dilution at 4 °C, washed 3× with PBS for 10 min, and appropriate secondary antibody dilutions were added for 2 h. Primary antibodies used on spinal cord tissue were βIII-tubulin (Covance, 1:2000), NeuN (Chemicon, mab377. 1:1000) or VGLUT-1 (Synaptic Systems #135303, 1:1000); secondary antibodies were goat anti-rabbit Alexa Fluor 488 (LifeTech #A11088, 1:500), goat anti-mouse Cy3 (Jackson Immunoresearch Labs #115–166,006, 1:400) or goat anti-mouse Alexa Fluor 568 (LifeTech #11031, 1:400). After three 10 min washes with PBS, sections were mounted onto slides and coverslipped with ProLong® Diamond Antifade Mountant (Thermofisher Scientific).

2.8. Quantification and characterization of regenerating FG labeled neurons in the DRG

From every experimental animal, three pairs of DRG were collected (L4-L6). In initial trials, sections were obtained from all ganglia; consistent with previous studies it was found that heavy and consistent retrograde FG label was always present in the sections from L5 ganglia (Swett et al., 1991). Thus, L5 DRGs from all rats that had received peroneal grafts were sectioned, immunostained and quantified. Some DRG neurons in L5 that projected into the peroneal branch may have

survived the initial injury but did not regenerate their axon successfully through and beyond the graft. Other neurons would have had axons that did not project into the peroneal branch and therefore were not injured when the grafts were inserted. These neurons would also not have been labeled by the peroneal FG injections. For these reasons only FG^+ neurons were analyzed and no attempt was made to count the total number of DRG neurons labeled with a particular antibody or combination of antibodies in the sectioned L5 material.

Prior to quantification slides were coded so that counts were done 'blind'. DRG sections with FG and double-labeled with IB_4/TrkA and CGRP/TrkC were photographed at x10 with a Nikon Eclipse E800 microscope using a QuantiFIRE camera operated by PictureFrame™ software (Optronics). All FG^+ cellular profiles in every section were manually counted using Image-Pro Express software (MediaCybernetics). These counts were saved and overlaid on images of the same sections stained with each of the primary antibodies, and only the FG labeled profiles were counted. Sections double-labeled with CNTFRα/p75 were counted directly under the microscope, switching between filters. In at least 5 tissue sections up to 11 fields, each measuring 243x243μm were counted. For this analysis, counts were expressed as a proportion of the total number of FG^+ neurons, and data were statistically analyzed with either one-way analysis of variance with least significant difference (LSD) post-hoc tests or with Kruskal-Wallis with Dunn's post-hoc tests and all pairwise comparisons, always with significance levels at $p < .05$. The number of samples and the power of statistical tests are indicated in the text.

2.9. Quantification of regenerate $ChAT^+$ axons in PN grafts

The number of $ChAT^+$ axons was quantified from longitudinal sections. Three longitudinal sections of normal nerve, and from each PN graft (3–4 animals per group), were viewed using a Nikon Eclipse E400 microscope and photographed at 20× magnification along the length of the section from the proximal to distal end. The sections were selected from across the breadth of the nerve to provide a representative sample of the nerve cross section. The numbers of stained axons crossing arbitrarily placed lines located in proximal, middle and distal parts of each nerve were counted and at each measurement site were averaged per 500 μm width of sectioned nerve. For each group, the nerve width at each measurement site was also measured to estimate the total number of $ChAT^+$ axons present at each location (Godinho et al., 2013; Krishnan et al., 2016). $ChAT^+$ axon counts per 500 μm width from all three sample locations from each animal per group were then combined to give an overall average of axons per unit graft width. For each group the number of immunostained $ChAT^+$ axons in longitudinal PN grafts was compared and analyzed using Kruskal-Wallis with Dunn's post-hoc tests and all pairwise comparisons, with a significance level $p < .05$.

2.10. Quantification and characterization of FG labeled motor neurons in the lumbar ventral horn

To eliminate the chance of double counting, every 6th 40 μm thick cross section of the spinal cord was used for quantification of retrogradely labeled FG^+ motor neurons in the 7 analyzed groups. Collection of sections began in upper lumbar cord and continued through to the upper sacral region in order to include the likely area of interest, *i.e.* segments L4 to L6. All sections with FG^+ motor neurons were photographed on a Nikon Eclipse E800 microscope using a Nikon DS-Qi2 camera at 2 different magnifications (x4 and x20), and in some cases at x40. Images were obtained as quickly as possible to minimize light-exposure and fading of the FG stain, enabling subsequent live counting of all FG^+ neurons in each section. Photographs were taken at the focal plane when the majority of nuclei were in focus and taken using two different filters to permit exclusion of autofluorescent profiles. The x4 magnification was used to obtain an overview of the whole FG stained region, whereas 20× and 40× objectives were used for the quantification and evaluation of cell body and nuclear dimensions. The analysis involved measuring the area (and equivalent diameter, a theoretical diameter of an even sphere generated from the areal measurement) of the somas and nuclei of non-counterstained FG^+ motor neurons. All measurements were hand drawn using NIS Element Basic Research 4.5 software from the 20× or 40× magnification pictures. Only cells that were FG^+ and had a clear nucleus were drawn; a total of 1322 cells was analyzed (Table 1).

2.11. Proportion of FG^+ motor neurons that were also immunoreactive for NeuN

After counting the number of FG^+ motor neurons per experimental group, spinal cord sections containing the greatest number of retrogradely labeled motor neurons were selected for NeuN immunostaining. Three uninjured normal animals were analyzed (3–6 sections per animal) and four animals from each of the 6 experimental groups (3 sections per animal). The relative numbers of FG^+, either $NeuN^+$ or $NeuN^-$, motor neurons were then determined in each section, yielding the average percentage of $NeuN^-$ counts/section (674 motor neurons counted – Table 1). Unlike all other counts, these counts were not done 'blinded' to the observer.

2.12. Quantification of VGLUT-1 contacts on regenerating FG^+ motor neurons

Sections for the VGLUT-1 counts were double immunostained with VGLUT-1 and βIII-tubulin and were photographed in a similar manner to the quantification and measurement of FG^+ motor neurons. Note that images were taken only in the focal plane in which the nucleolus was in focus – and counts made solely from that image. We examined immunostained sections from three normal, autograft, acellular and LV NT-3 graft animals, and from four SC-GFP, LV-CNTF and LV-NGF animals; in total, 370 FG^+ motor neurons were analyzed (Table 1). Only

Table 1
Summary of the number of motor neurons in normal and experimental groups analyzed in each analysis.

Number of motor neurons (MN) included in each analysis								
Analysis	Normal nerve	Autografts	Acellular grafts	SC-GFP	SC-CNTF	SC-NGF	SC-NT-3	Total
FG^+ MN counts	807	702	607	690	741	471	563	4581
$NeuN^+$ counts	83	55	36	80	40	35	11	340
$NeuN^-$ counts	65	41	36	52	57	34	49	334
MN measurements	168	247	232	234	164	138	139	1322
MN with $VGLUT1^+$ 'contacts'	125	37	28	55	48	48	17	370

Summary of the number of motor neurons in normal and experimental groups analyzed in each analysis. FG, fluorogold. Columns headed SC-GFP, SC-CNTF, SC-NGF, SC-NT-3 denote PN grafts containing Schwann cells (SC) transduced with LV-GFP, LV-CNTF, LV-NGF and LV-NT-3 respectively.

VGLUT-1 terminals that were in very close apposition to FG^+ cells were counted (Liu et al., 2014; Krishnan et al., 2018). Statistical tests on motor neurons were made using GraphPad Prism v6.01, using Kruskal-Wallis analysis with pairwise comparisons followed by Dunn's multiple comparison tests, and significance levels set at $p < .05$.

3. Results

3.1. Analysis of regenerated dorsal root ganglia neurons

3.1.1. FG^+ neurons

Large numbers of FG^+ axons were seen within normal nerve and in all peroneal grafts (Fig. 2). For each experimental group, the numbers of FG-labeled cell bodies in L5 DRG (Fig. 3A-D) were manually quantified. Quantification was performed on two out of a series of five slides, therefore corresponding to roughly 40% of sections of the entire DRG. All FG^+ neurons were counted. Given that care was taken to ensure that FG was injected in host peroneal nerve distal to the grafts, only neurons with injured axons that regenerated and *projected beyond the grafts* were labeled. A Kruskal-Wallis test revealed significant differences between groups in the number of FG^+ profiles (χ^2 (8, n = 45) = 19.437, p = .013) (Fig. 4A). The average number of retrogradely labeled FG^+ neurons after injection into normal peroneal nerve was higher than in any experimental group, the 'gold standard' autograft group being next highest. The lowest average number of FG-labeled neurons was seen in the GDNF graft group (56.8), corresponding to a 2.5-fold decrease from normal numbers and 1.95-fold decrease from the number of profiles in the autograft group. A Dunn's post-hoc test with all pairwise comparisons indicated that the number of FG^+ DRG neurons in the GDNF group was significantly lower than in the normal group ($p < .05$) (Fig. 4A), although not significantly different from other reconstituted graft groups, including the control SC-GFP group.

3.1.2. $CGRP^+$ neurons

From each of the control (ungrafted normal) animals and experimental groups (n = 5), between 10 and 13 sections, comprising about 20% of the L5 DRG, were immunostained for calcitonin-gene related peptide (CGRP) (Fig. 3A,B). Neurons that were FG^+ and $CGRP^+$ were counted and expressed as a percentage of the total number of FG^+ neurons in those sections (Fig. 4B). The proportion of $CGRP^+$ regenerating neurons ranged from about 20% in acellular and LV-GFP grafts to about 40% in grafts containing NT-3 transduced SCs. A one-way analysis of variance comparing mean percentages revealed significant differences between experimental groups (F (8, 36) = 6.431,

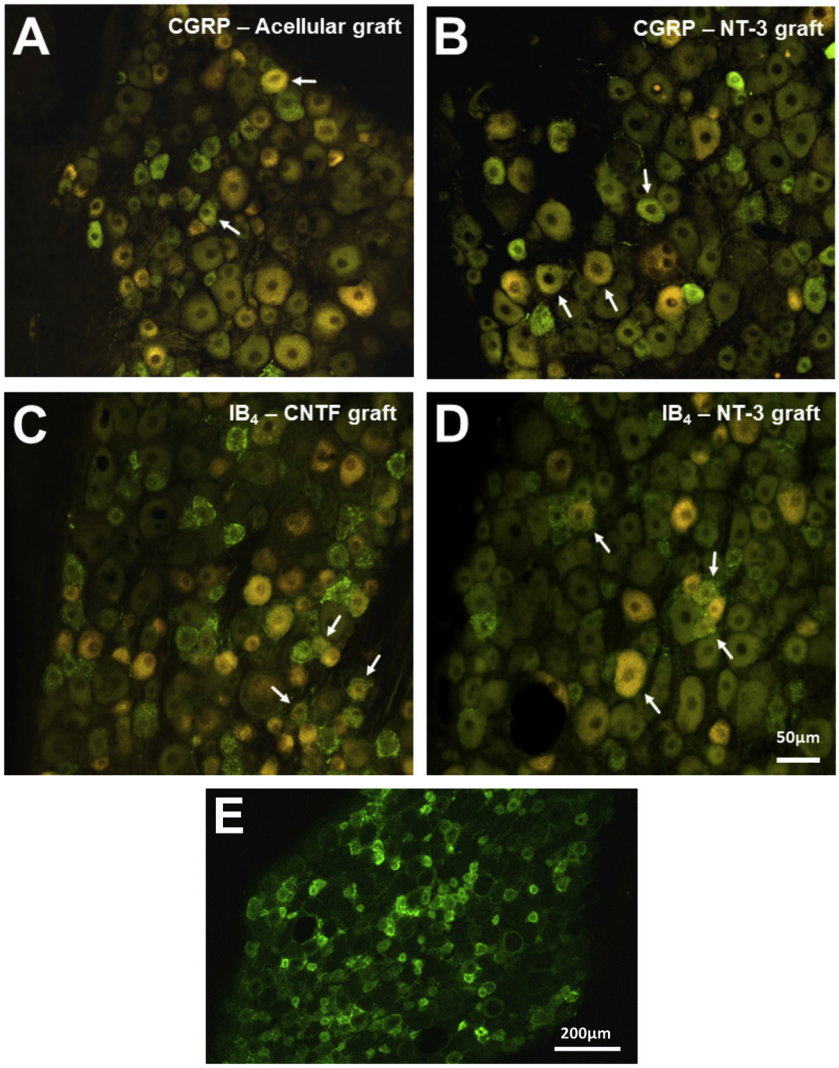

Fig. 3. Examples of L5 dorsal root ganglion (DRG) neurons retrogradely labeled with FluoroGold (FG) after injections into host peroneal nerve distal to grafts. DRG sections from rat with acellular graft (A) and rat with graft containing LV-NT-3 modified Schwann cells (B) immunostained with an antibody to CGRP. C, D, IB_4 immunostained DRG sections from animals with grafts containing LV-CNTF and LV-NT-3 modified Schwann cells respectively. Arrows point to examples of immunopositive, FG labeled neurons. E, IB_4 immunostained section; note pericellular rings around many neurons. Scale bar for A-D = 50 µm, E = 200 µm.

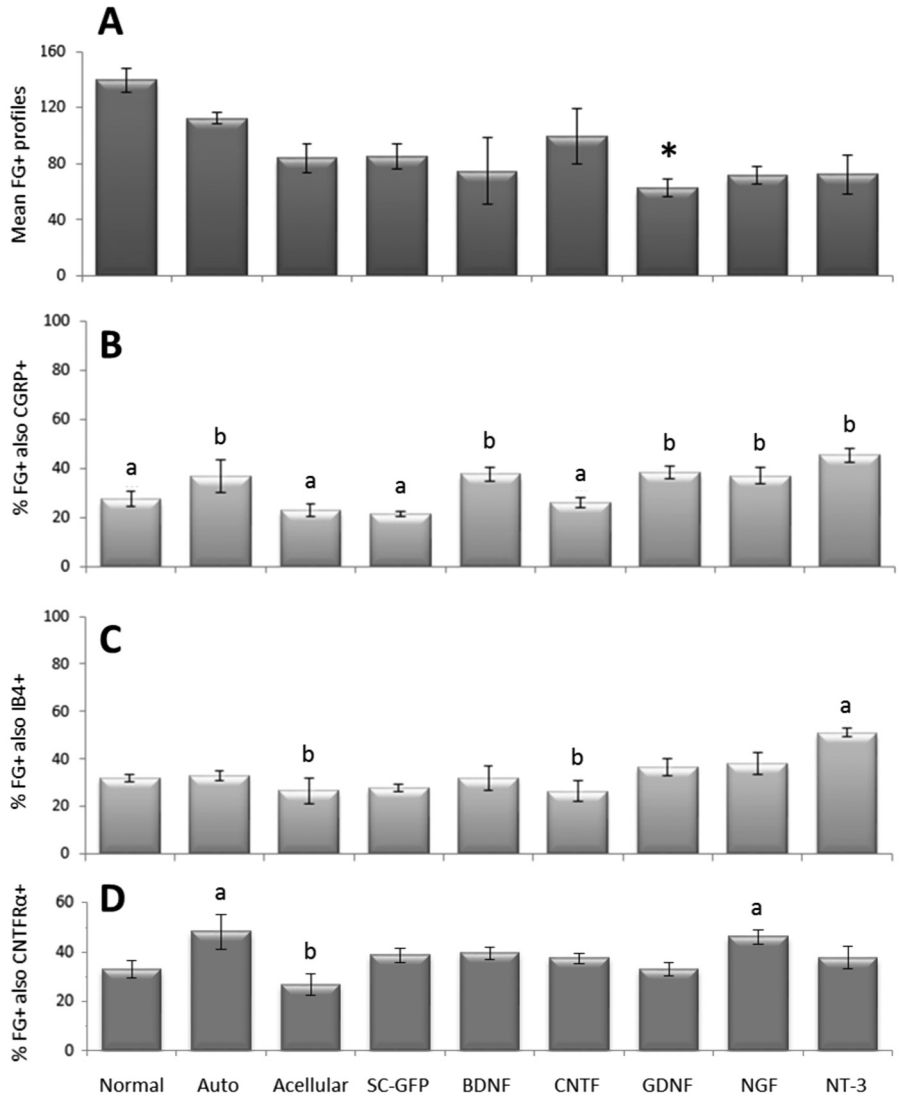

Fig. 4. A, mean number (± SEM) of FluoroGold (FG) labeled neurons in L5 dorsal root ganglia (DRG) in each experimental group. There were significantly less profiles in the LV-GDNF group compared to the normal uninjured group (asterisk, $p < .05$). B-D, the mean percentage (± SEM) of FG labeled DRG neurons immunopositive (+) for CGRP (B), IB_4 (C) and CNTFRα (D). B, proportion of FG labeled neurons that were were $CGRP^+$ in normal nerves, acellular, SC-GFP and CNTF nerve grafted groups (a) was significantly less ($p < .05$) than the mean percentage in autografts, and grafts containing Schwann cell engineered to express BDNF, GDNF, NGF or NT3 (b). C, proportion of FG-labeled profiles that were IB_4^+ in the NT3 group was significantly higher than in all other groups (a), and in the acellular and CNTF groups was significantly lower than the NGF group (b) (both a and b, $p < .05$). D, the proportion of FG labeled expressing CNTFRα in autografts and the NGF group (a) was significantly higher than in normal, acellular and GDNF groups. In the acellular group (b), the proportion was significantly lower than in autografts, SC-GFP, BDNF and NGF groups (all $p < .05$).

$p < .0005$). The mean percentage of FG-labeled neurons that were also $CGRP^+$ in L5 DRG connected to normal nerves, acellular, SC-GFP and CNTF nerve grafted groups (a, Fig. 4B) was significantly less ($p < .05$) than the mean percentage in autografts, and BDNF, GDNF, NGF and NT-3 graft groups (b, Fig. 4B). The mean percentages in the DRG from acellular and SC-GFP groups were also significantly lower ($p < .05$) compared to all neurotrophic groups, with the exception of the group containing LV-CNTF transduced SCs. Thus the regrowth of this subpopulation of sensory axons through SC reconstituted grafts is stimulated by gene therapy for neurotrophins, with the exception of CNTF. The data therefore suggest that neurotrophic factor gene therapy is beneficial for the regeneration of $CGRP^+$ axons.

3.1.3. IB_4^+ neurons

Another set of sections from each group, again comprising about 20% of the L5 DRG, were immunostained with antibodies to IB_4 (Fig. 3C,D). With this antibody, in all experimental groups IB_4^+ pericellular ring-like profiles were commonly seen around neurons (Fig. 3E), likely associated with neuronal sprouts and satellite glial cells (Li and Zhou, 2001). IB_4^+ neurons in each group were expressed as a percentage of the FG^+ neurons that had regenerated axons into distal peroneal nerve (Fig. 4C). The mean percentages were compared using a one-way analysis of variance, indicating a significant difference between groups ($F(8, 36) = 4.509$, $p = .001$). One-way analysis of variance with LSD post-hoc comparisons revealed that the proportion of IB_4^+ neurons in DRG from NT-3 grafted rats (about 50%) was significantly higher ($p < .05$) than all other groups (a, Fig. 4C). Additionally, both the mean percentage of IB_4^+ neurons in DRG from acellular and CNTF groups (b) was significantly lower ($p < .05$) compared to the NGF group.

3.1.4. $CNTFR\alpha^+$ and $p75^+$ neurons

A third set of sections from 3 of the 5 animals in each group was double-labeled with antibodies to the CNTFRα receptor and p75 neurotrophin receptor. p75 is co-expressed with most Trk receptor expressing DRG neurons (Wright and Snider, 1995), and CNTFRα is present on most DRG neurons (MacLennan et al., 1996). Unlike the analysis described above, in which all FG-labeled regenerated neurons were counted, in these sections, for each L5 DRG, counts were made in random fields from at least five tissue sections. Depending on DRG size, from 7 to 11 fields (each measuring 243 × 243 μm) were counted per DRG section. In agreement with earlier work (Stucky and Koltzenburg, 1997) about 50% of normal DRG neurons expressed p75. In injured animals, antibodies to p75 labeled ring-like structures around some DRG neurons (Zhou et al., 1996), especially those of larger diameter. The numbers of FG^+ neurons that were $CNTFR\alpha^+$ were counted and expressed as a percentage of the total number of FG^+ profiles (Fig. 4D). A one-way analysis of variance revealed significant differences between

experimental groups (F (8, 18) = 2.824, p = .032). Post-hoc comparisons revealed that DRGs from autograft and NGF groups contained significantly more ($p < .05$) regenerating CNTFRα$^+$ neurons compared to normal, acellular and GDNF groups (a, Fig. 4D), and the proportion of CNTFRα$^+$ neurons was significantly lower ($p < .05$) in acellular compared to BDNF and SC-GFP groups (b, Fig. 4D). The proportion of regenerating neurons that were CNTFRα$^+$/p75$^+$ did not significantly differ between groups.

3.1.5. TrkA$^+$ or TrkC$^+$ neurons

Distinct subpopulations of DRG neurons express TrkA, TrkB or TrkC (Wright and Snider, 1995). Due to the limited number of sections available per DRG, the set of sections immunostained with IB_4 was also immunostained with a TrkA antibody, and those sections immunostained with CGRP were also immunostained with a TrkC antibody. Counts of TrkA$^+$ neurons in normal controls and each experimental group were compared using a Kruskal-Wallis test, which revealed no significant differences (χ^2 (8, n = 45) = 0.980, p = .998). Similarly, there were no statistically significant differences between groups in the mean percentage of regenerated neurons expressing TrkC (F (8, 36) = 1.225, p = .313).

3.2. Morphological assessment in longitudinal sections of grafts

Longitudinal sections of grafts allowed the monitoring of transgene expression by transplanted SCs and the uptake and retrograde transport of FG (Fig. 2). In addition, it was possible to qualitatively assess the effects of neurotrophic factors on host axon growth and donor graft morphology. As observed before (Godinho et al., 2013), the labelling of SCs with LV-GFP confirmed continued transgene expression within grafts for at least 10 weeks (not shown). All PN sheaths were reconstituted *in vitro* with SCs in exactly the same way, yet post-transplantation there were considerable differences in graft and axon morphology that depended on the particular growth factor expressed by the genetically modified glia. We previously documented changes in graft width in PN containing different donor SC populations, and in some grafts (*e.g.* with cells engineered to express BDNF or NT-3) there was clear fasciculation (Godinho et al., 2013). In the present study, when compared to normal PN (Fig. 5A), in LV-NGF grafts and especially in LV-GDNF grafts (Fig. 5B), fascicles of often disorganised βIII-tubulin$^+$ fibers were evident, indicating that axons were clearly losing their orientation and longitudinal organisation. Such axonal entrapments (see also Hoyng et al., 2014) were not obvious in grafts with SCs engineered to express BDNF, CNTF or NT-3.

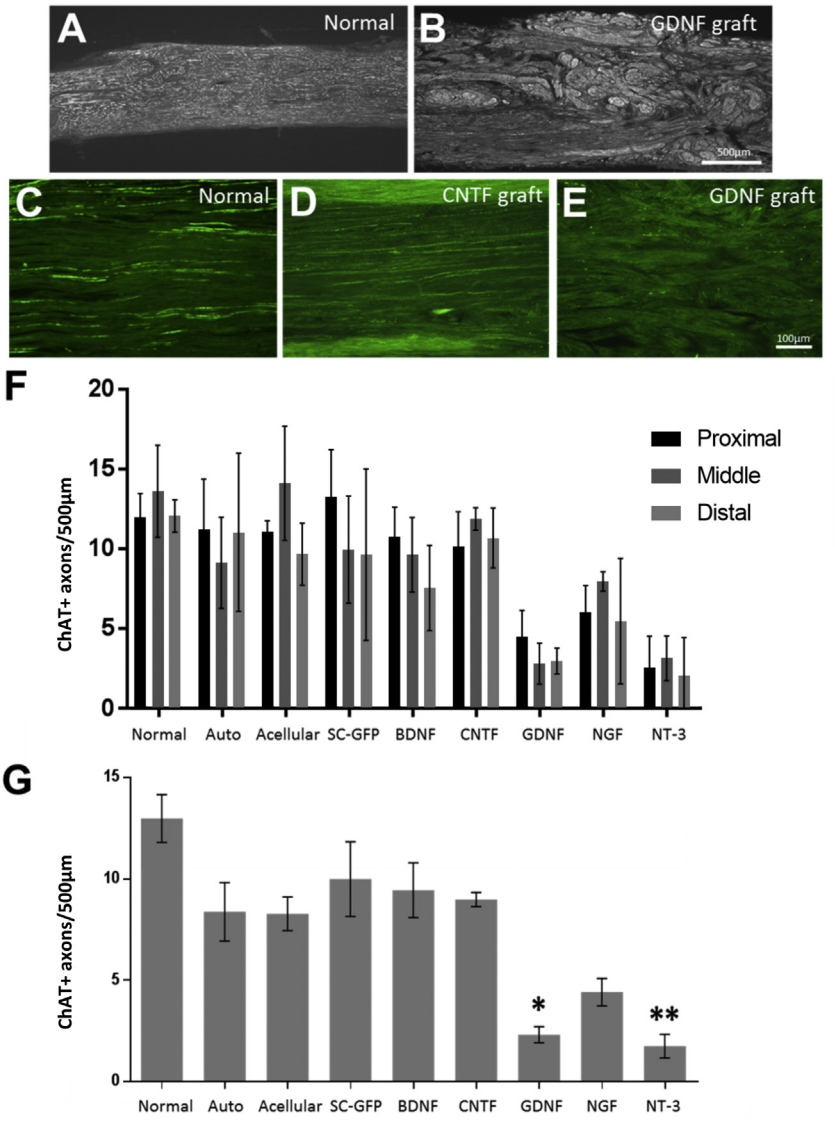

Fig. 5. A-B, longitudinal sections of normal peroneal nerve (A) and graft containing Schwann cells engineered to express GDNF (B). immunostained with an antibody to βIII-tubulin. Note the disorganized appearance and thickness of the GDNF graft. C-E, longitudinal sections of normal nerve (C), CNTF engineered graft (D) and GDNF graft (E) immunostained with an antibody to choline acetyl transferase (ChAT). Scale bars: A, B = 500 µm; C-E = 100 µm. F, average number (± SEM) of ChAT positive axons per 500 µm width of nerve, measured at three locations. G, average number (± SEM) pooled from counts shown in F. All graft groups contained fewer axons than normal nerves, and compared to normal nerves there were significantly fewer ChAT positive axons in GDNF ($p < .05$) and NT-3 ($p < .01$) engineered grafts.

3.3. ChAT immunoreactive axons in PN grafts

In an earlier study, grafts reconstituted with genetically modified SCs were immunostained for markers of sensory axons – CGRP and IB_4 (Godinho et al., 2013). Here, to provide information more focused on the presence of regenerating efferent motor axons, PN graft sections were immunostained with antibodies to central ChAT (examples shown in Fig. 5C-E). Note again the characteristic disorganized fascicular nature of graft organization in the LV-GDNF engineered material (Fig. 5E). Three to four nerves were sampled from each group, at each of three locations within the grafts – proximal, middle and distal (Fig. 5F). The number of $ChAT^+$ axons was estimated per 500 μm width of each graft and the numbers averaged at each location. No significant difference in number was seen from proximal to distal in any group, but grafts containing SCs engineered to express either GDNF, NGF or NT-3 consistently contained fewer $ChAT^+$ profiles. This was especially obvious in grafts containing SCs transduced with GDNF or NT-3, the low numbers in proximal regions indicating an initial lack of penetration into the grafts. $ChAT^+$ axon counts per 500 μm nerve width from all three sample locations were then combined to give an overall average count of axons per unit graft width (Fig. 5G). Transplanted animals contained fewer axons in the PN grafts than normal nerves, but in most cases this decrease was not significant; however compared to normal nerves there were significantly fewer $ChAT^+$ axons in the GDNF ($p = .021$) and NT-3 ($p = .009$) engineered grafts (asterisk, Fig. 5G).

3.4. Graft thickness and estimates of total number of $ChAT^+$ axons

Grafts were generally thicker compared to normal peroneal nerve. In particular, measurement of graft width in longitudinal sections (Fig. 5A, B) revealed that grafts containing GDNF ($p = .045$) and NT-3 ($p = .032$) engineered SCs were significantly wider than normal nerve (Fig. 6A), the latter consistent with our earlier study (Godinho et al., 2013). The expanded girth of these reconstituted grafts was associated with significantly increased size of the proximal peroneal nerve stumps attached to the grafts (data not shown). Based on the graft width measurements, in each graft group it was possible to estimate the average total number of $ChAT^+$ axons counted at graft location and relate this estimate to the average thickness of each graft (Fig. 6B). The lowest counts were seen in the LV-NGF and especially LV-GDNF and LV-NT-3 groups, and highest in normal nerve. Note that acellular grafts were of similar thickness to the aforementioned genetically modified grafts, yet on average contained many more $ChAT^+$ profiles.

3.5. Analysis of regenerated motor neurons in ventral horn of the spinal cord

3.5.1. FG^+ neurons

Retrogradely labeled, regenerating FG^+ motor neurons were readily visible in the ventral horn from normal Fischer rats (arrow, Fig. 7A,C), with fewer cells visible in experimental PN grafted animals (Fig. 7B). Counts were made from every 6th, 40 μm thick, section containing FG^+ neurons cells in L4-L6 ventral horn of the lumbar spinal cord. In 34

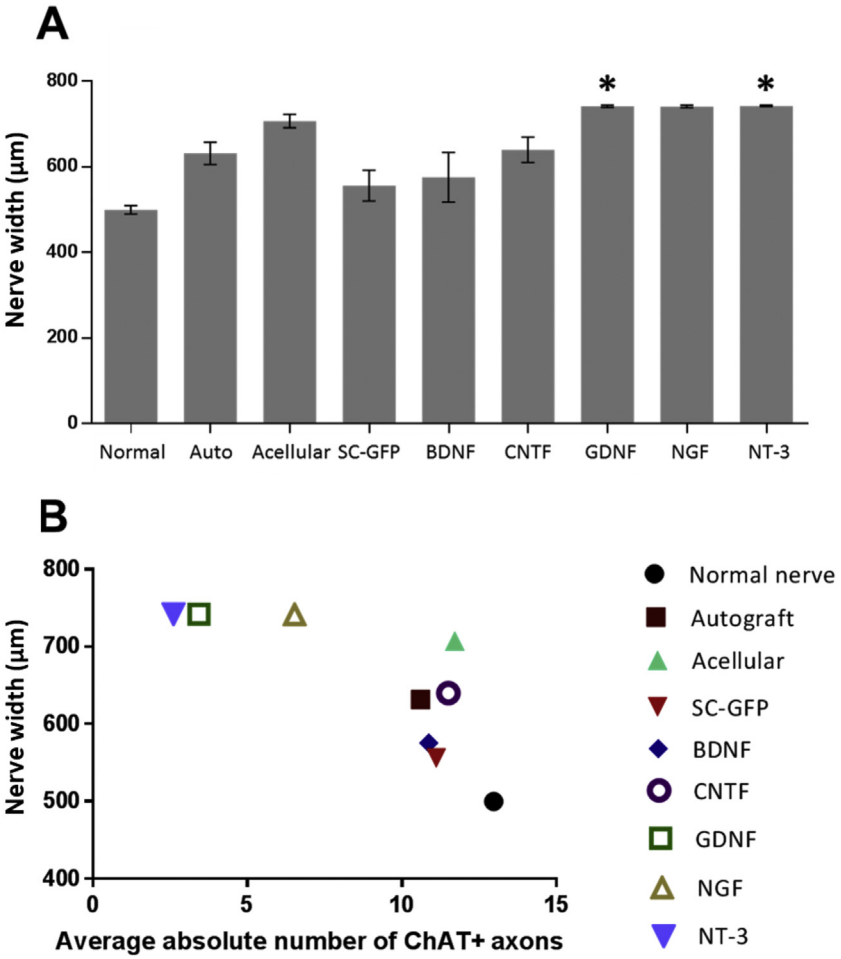

Fig. 6. A, Average nerve width (± SEM) of normal peroneal nerve and each of the experimental graft groups. Grafts containing GDNF and NT-3 engineered Schwann cells were significantly wider than normal nerve (asterisks, $p < .05$). B, estimated average total number of ChAT positive axons plotted against average width of each graft. Note the displaced position of the LV-NT-3, LV-GDNF and LV-NGF groups.

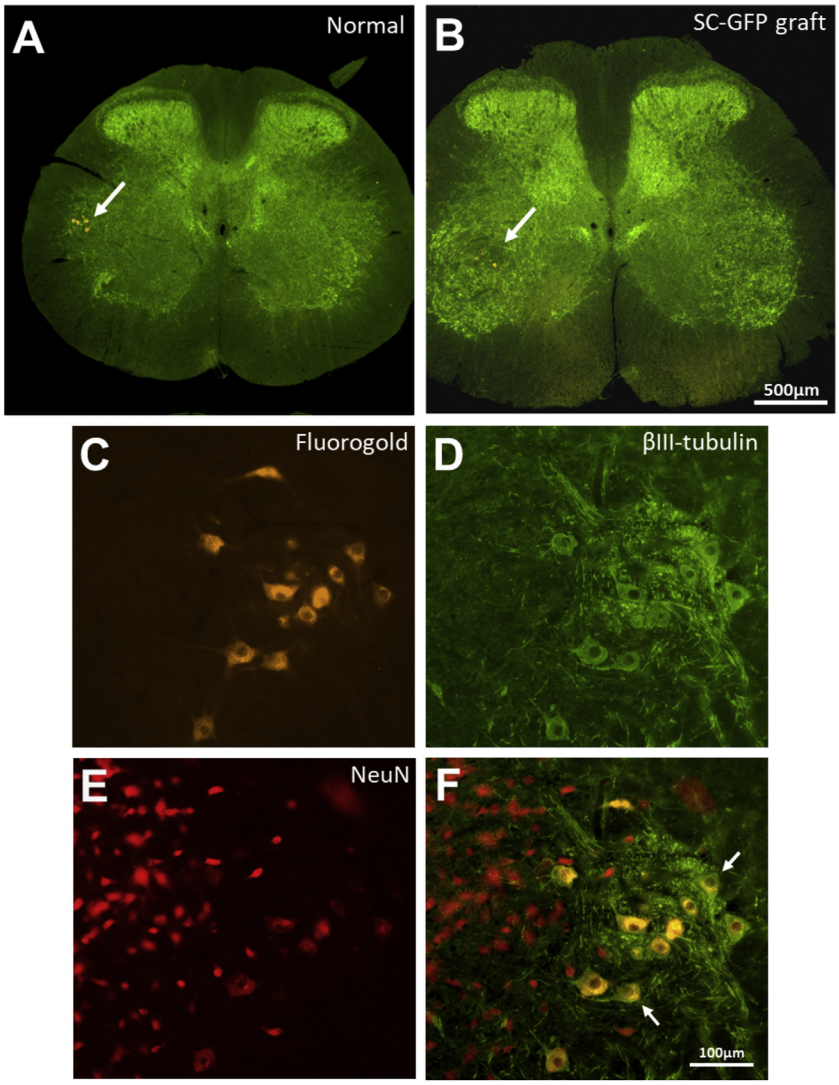

Fig. 7. A-B, low power images of transverse spinal cord sections immunostained for VGLUT1 (green) from uninjured control (A) and an animal that had received a graft containing Schwann cells expressing green fluorescent protein (B). FluoroGold (FG) labeled neurons are arrowed – note the reduced number in the graft animal. C-E, a spinal cord section from a normal rat showing (C) FG labeled neurons, (D) same field immunostained for βIII-tubulin, (E) same field immunostained for NeuN, and (F) all three images combined. NeuN negative, FG labeled motor neurons are arrowed. Scale bars: A, B = 500 µm; C-F = 100 µm. (For interpretation of the references to colour in this figure legend, the reader is referred to the web version of this article.)

animals (n = 5/group, except normal nerve n = 4) from seven groups (normal nerve, autograft, acellular, SC-GFP, CNTF, NGF, NT-3) a total of 4581 FG^+ positive cells were counted (Table 1). These counts were carried out 'blind' to the experimental group. As expected, the normal (uninjured) nerve group showed the highest FG^+ cell count, however subsequent analysis of FG^+ motor neuron counts/section did not show any significant differences based on Kruskal-Wallis (p = .871) followed by a Dunn's multiple comparison, between any of the experimental groups (Fig. 8A). Note that, given the low numbers of regenerate $ChAT^+$ axons within the transplanted nerve in the NT-3 engineered graft group (Fig. 5G), FG^+ motor neuron counts in the spinal cord were higher than might be expected (Fig. 8A).

3.5.2. Morphological assessment of regenerated FG^+ motor neurons

A total of 356 images, using a blinded allocated numbering scheme, were randomly taken in order to measure soma and nucleus size of the FG^+ cells in the seven groups (normal nerve, autograft, acellular, SC-GFP, CNTF, NGF, NT-3). A total number of 1322 FG^+ motor neurons was measured (Table 1). Labeled motor neurons in normal animals showed a tendency for allocation to two groups, one of smaller equivalent diameter peaking around 29–30 µm and one of larger equivalent diameter peaking around 42–43 µm. The mean soma areas for FG^+ motor neurons appeared to be greater in normal animals than in any of the experimental groups (Fig. 8B), although due to a large amount of variance (and perhaps differential regeneration of α and γ motor neurons of characteristically different size range – see below) this difference was not significant (both soma and nucleus, p = .99).

3.5.3. Analysis of NeuN expression in regenerated FG^+ motor neurons

The neuronal DNA binding protein NeuN has been reported to be expressed in α- but not γ-motor neurons (Mullen et al., 1992; Friese et al., 2009), innervating extrafusal and intrafusal muscle fibers respectively. Quantitative counts (a total of 674 neurons) were therefore made of regenerating FG^+, $\beta III\text{-tubulin}^+$ neurons that were either immunopositive or negative for NeuN (Table 1, Fig. 7C-F). While the average total number of FG^+ motor neurons was similar across all groups (Fig. 8A), a significantly higher proportion of these regenerating neurons was NeuN negative ($NeuN^-$) in the graft group with NT-3 engineered SCs (Fig. 9). The percentage of retrogradely labeled $NeuN^-$ neurons in the NT-3 group (82%) was about double that seen in normal uninjured rats (44%). Statistical analysis revealed that the percentage of FG^+ motor neurons that were $NeuN^-$ was significantly less in the SC-GFP group than in the NT-3 group (asterisk, Fig. 9) - Kruskal-Wallis analysis (p = .024) followed by a Dunn's multiple comparison (p = .035). Thus NT-3 appeared to preferentially enhance the regeneration of γ-motor neurons.

3.6. VGLUT-1 expression in spinal cord

VGLUT-1 is reported to be a marker for the terminals of primary 1a

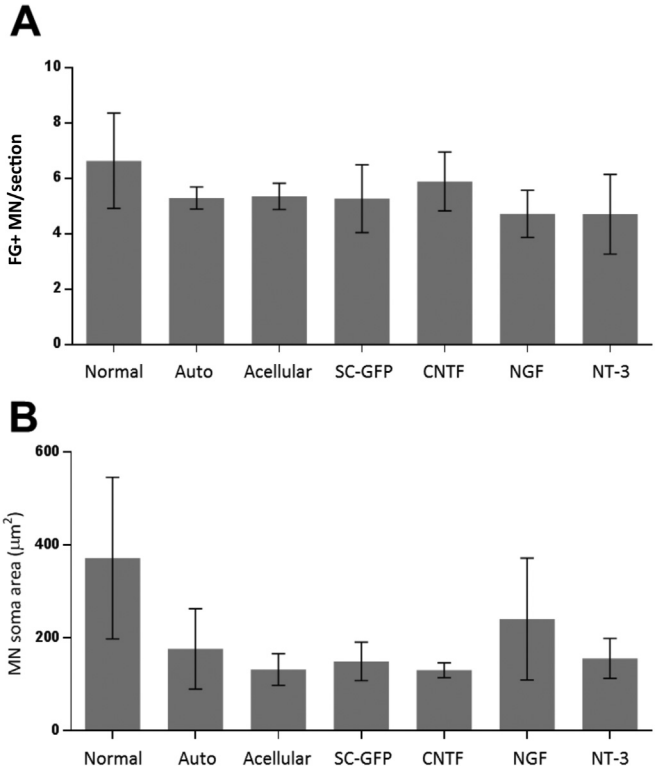

Fig. 8. A, average number (mean ± SEM) per section of FluoroGold (FG) labeled motor neurons in the ventral horn of spinal cord segments L4-L6. B, average (± SEM) soma area of regenerated FG labeled motor neurons in each of the seven surveyed groups.

afferents originating from muscle spindles (Todd et al., 2003; Levine et al., 2014; Liu et al., 2014). There was high expression of VGLUT-1 in the ventral horn of the spinal cord in normal animals (Fig. 7A, Fig. 10A), however the number of VGLUT-1$^+$ profiles was clearly reduced in localized regions of the ventral horn ipsilateral to all PN grafts (*e.g.* spinal cord from SC-GFP grafted animal, Fig. 7B). The white arrows in Fig. 10 A,B point to examples of VGLUT-1 terminals in close apposition to the soma of large βIII-tubulin immunolabeled, presumably α motor neurons. For each group, the number of these VGLUT-1$^+$ profiles per neuron was counted in an image plane in which the nucleolus was clearly in focus. On average, compared to uninjured controls the number of apparent VGLUT1 terminal contacts on motor neurons was less in all SC graft groups (Fig. 10C), but only in the acellular group was this loss of connectivity significant, (Kruskal-Wallis, $p = .058$) followed by Dunn's multiple comparison (adjusted $p = .041$). It is important to note that in all graft groups, most frequently seen in animals with SC-NT-3 grafts, there were occasional VGLUT-1 contacts with regenerating FG$^+$ neurons (arrows, Fig. 10B), indicating the restoration of at least some sensory-motor relays after nerve reconstruction.

4. Discussion

The research described here is an extension of an earlier morphological and behavioural study that used allogeneic PN sheaths repopulated *ex vivo* with congeneic SCs genetically modified to express neurotrophic factors to repair a 1 cm defect in rat peroneal nerves (Godinho et al., 2013). In the present study, using this model, we injected the retrograde tracer FG into peroneal nerve distal to PN grafts 10 weeks post-transplantation to quantify and phenotype regenerating sensory and motor neurons. Two additional LV vectors were tested, expressing either GDNF or NGF. Outcomes were complex, and effects on sensory and motor neurons varied depending on the trophic factor engineered into donor SCs. While graft groups contained fewer FG$^+$ DRG neurons than non-operated controls, there was a trend for this loss to be less in autograft and LV-CNTF groups, and the decrease was only significant in the LV-GDNF group. These grafts had a complex fascicular morphology that may have resulted in axon trapping. A significantly higher proportion of CGRP$^+$ neurons was seen in autografts and most neurotrophic factor groups compared to LV-GFP and acellular groups, and there were more IB_4^+ neurons in DRGs from the NT-3 group. However, compared to normal nerves, there were significantly fewer ChAT$^+$ axons in grafts containing SCs expressing NT-3 or GDNF. In ventral horn, the overall number of FG$^+$ motor neurons per section was similar in all groups, however the proportion of NeuN$^-$, FG$^+$ neurons - generally between 40 and 45% - was almost doubled in the NT-3 group (82%). VGLUT-1$^+$ terminals in 'contact' with regenerating FG$^+$ α-motor neurons were occasionally seen in PN grafted animals, with a trend for more such contacts in neurotrophin expressing grafts.

As described previously (Godinho et al., 2013), 10 weeks after transplantation there were marked differences between experimental groups in the general morphology and architecture of grafts. All grafts appeared to be thicker than normal peroneal nerve, with NT-3 and GDNF grafts significantly greater in size than uninjured nerve. This in turn was associated with an increase in the size of the proximal peroneal nerve stumps attached to the grafted material. Interestingly, autografts of sciatic nerve injected with LV-GDNF, an approach that transduces not only SCs but other non-neuronal cells in the grafted material, were also found to be much larger (Hoyng et al., 2014). Note here that sustained vector-mediated delivery of these various

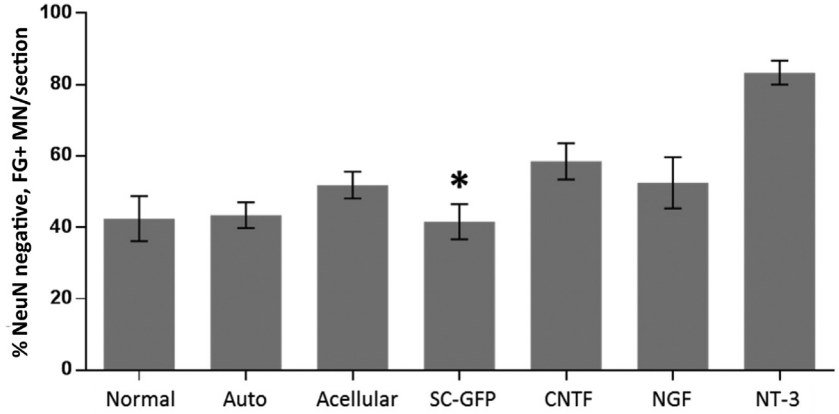

Fig. 9. The average percentage (± SEM) of FluoroGold labeled neurons per lumbar spinal cord section that were not immunoreactive for NeuN. The proportion of NeuN negative neurons in the Schwann cell-GFP was significantly less than the NT-3 group (asterisk, $p < .05$).

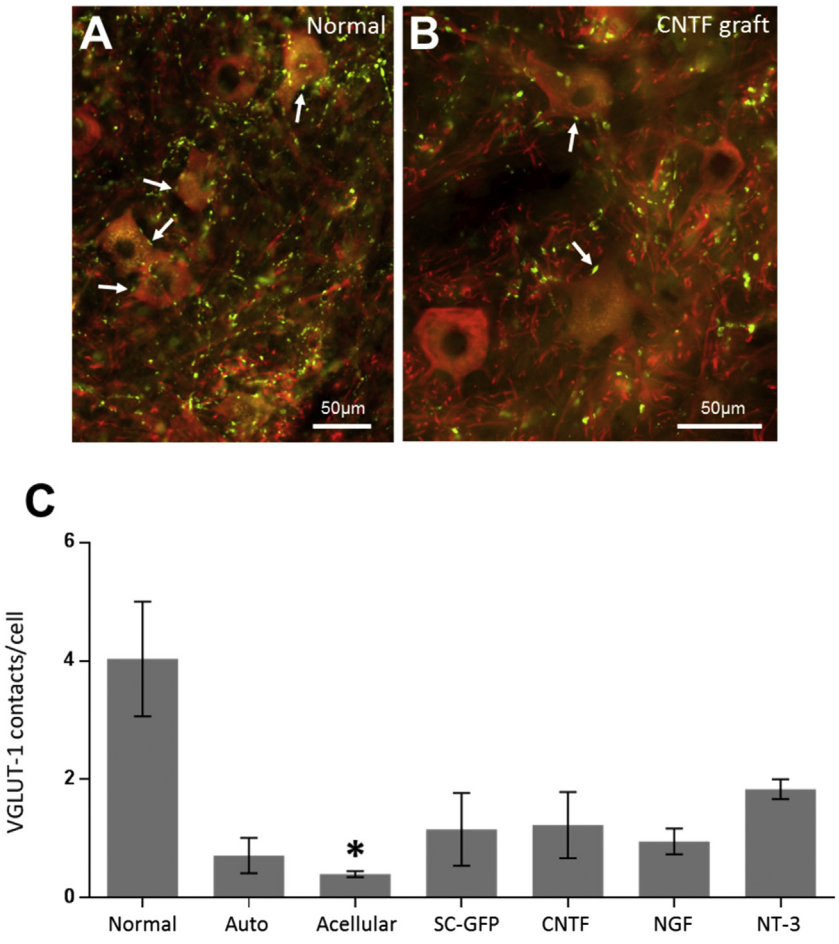

Fig. 10. A-B, high power images of sections immunostained for βIII-tubulin (red) and VGLUT1 (green). There are many more VGLUT-1 terminals in close apposition to the soma of large βIII-tubulin immunolabeled, presumably α motor neurons (white arrows), in normal animals (A) compared to grafted rats (B, LV-CNTF group). Scale for A and B = 50 μm. C, the average number (± SEM) of VGLUT-1 positive contacts per neuron, counted in an image plane in which the nucleolus is in focus. The number in the acellular group was significantly less than normal control (asterisk, $p < .05$). (For interpretation of the references to colour in this figure legend, the reader is referred to the web version of this article.)

neurotrophic factors may also have induced different amounts of SC proliferation after transplantation (Hoyng et al., 2014) or altered the phenotype of infiltrating cells such as fibroblasts or macrophages. There was also likely intermixing of SCs between graft and host (Symons et al., 2001), the emigration of engineered, congeneic SCs into distal host peroneal nerve potentially enhancing axon regrowth beyond the PN bridge.

Previous immunohistochemical and ultrastructural analysis revealed macrophage infiltration, extracellular matrix deposition and fascicularization of axon bundles in grafts containing SCs transduced with growth factors (Godinho et al., 2013). Fascicles were especially evident in grafts containing BDNF or NT-3 expressing SCs. The amount of myelination of regrown axons also differed between groups, grafts with BDNF expressing SCs having the highest ratio of myelinated to unmyelinated fibers, NT-3 grafts containing many more unmyelinated axons (Godinho et al., 2013). In the present study, the organization of BDNF and CNTF engineered grafts appeared relatively normal, with linearly ordered profiles, compared to grafts containing SCs engineered to express NGF or GDNF which displayed a highly irregular morphology. It seems likely that this neuroma-like architecture compromised sustained, longitudinal axonal regeneration along the grafts, perhaps entrapping many regenerating fibers (Eggers et al., 2008; Tannemaat et al., 2008; Santosa et al., 2013; Hoyng et al., 2014). In this regard, it is of interest that NGF levels have been linked to neuromas (Atherton et al., 2006) which in turn have been reported to express receptors for both NGF and GDNF (Harpf et al., 2002). It is important to emphasize that all donor sheaths were reconstituted *in vitro* with SCs in exactly the same way prior to engraftment. Given that all cellular grafts were similarly constructed, the SCs seeded into randomly selected freeze-thawed nerve sheaths, it is remarkable how graft morphology subsequently varied so consistently and so extensively with the type of transgene incorporated into the donor cells (see also Godinho et al., 2013). These differences were seen throughout the length of the grafts, not just at host-graft interfaces.

4.1. Sensory neurons

In the analysis of lumbar DRGs, as expected the highest mean number of FG-labeled neurons was found in the normal group. Of the engineered grafts, although not significant at $p < .05$, the number of FG^+ neurons was greatest in animals with grafts containing SCs transduced with CNTF. This is consistent with previous studies describing trophic effects of CNTF on injured DRG neurons (Lo et al., 1995; Sango et al., 2008), but differs somewhat from our previous study (Godinho et al., 2013), in which the number of βIII-tubulin$^+$ axons per mm width of nerve grafts was comparatively low in CNTF engineered grafts. In contrast, the total number of FG-labeled neurons in the GDNF group was significantly reduced, consistent with the observation that grafts containing GDNF transduced SCs possessed bulbous structures and a highly disorganized architecture that almost certainly impeded the linear regenerative growth of axons within the grafts. Note here that the overall impact of the release of neurotrophic factors from genetically modified SCs in peroneal grafts needs to be viewed in light of the observation that at least some DRG neurons can increase endogenous neurotrophin expression after axotomy (Gordon, 2009; Richner et al., 2014), and satellite cells in the DRG can also upregulate factors such as NGF and NT3 (Zhou et al., 1999) or GDNF (Hammarberg et al., 1996) after injury.

Alternate series of L5 DRG sections were co-immunostained for either IB_4/TrkA or CGRP/TrkC. Although TrkA has been reported to be

down regulated 7 days after sciatic nerve transection in mice (Kalous and Keast, 2010), in our experimental groups we found no significant differences in the proportion of FG^+ neurons that were TrkA or TrkC immunoreactive 10 weeks after surgery, perhaps reflecting recovery of expression during the regenerative process (Richner et al., 2014). Sections were also co-stained for the receptors CNTFRα and p75. $p75^+$ ring-like structures were seen around some FG^+ DRG neurons, especially noticeable around larger cells. Others have described similar structures after PN injury (Zhou et al., 1996) and this may be associated with expression in non-neuronal, satellite cells. For CNTFRα there was a significant difference between experimental groups; perhaps surprisingly, in the autograft and NGF but not the CNTF groups there was a significantly higher proportion of FG^+ neurons that were $CNTFR\alpha^+$ compared to normal, acellular and GDNF groups. After a PN lesion there is upregulation of CNTFRα in motor neurons (MacLennan et al., 1999), and there also is an increase in receptor expression in skeletal muscle which can promote regeneration of motor axons (Lee et al., 2013, 2019); however, to our knowledge, while message for this receptor is expressed in a great many DRG neurons (Ip et al., 1993), changes in expression levels during PN regeneration have not been described.

In the earlier study (Godinho et al., 2013), longitudinal graft sections were stained with antibodies to CGRP or IB4, markers typically used to characterize subpopulations of sensory neurons (Stucky and Lewin, 1999). CGRP labels medium and small-sized peptidergic neurons that give rise to thinly myelinated Aδ fibers and unmyelinated C fibers with mainly nociceptive properties (Ju et al., 1987; Tannemaat et al., 2008). These neurons express TrkA and p75, and have been shown to respond to NGF (Averill et al., 1995; Bennett et al., 1996 Michael et al., 1997). In the present study, 10 weeks after peroneal nerve repair there were significant differences between experimental groups regarding the proportion of FG^+ DRG neurons that were $CGRP^+$. Overall, there were significantly fewer $CGRP^+$ neurons in the normal, acellular, SC-GFP and CNTF groups compared to the autograft, BDNF, GDNF, NGF and NT-3 groups. In the earlier study, more $CGRP^+$ axons were seen in grafts containing NT-3 expressing SCs, although due to inter-animal variance this increase was not significant (Godinho et al., 2013). It seems possible that the trophic effects of the neurotrophins on CGRP expressing sensory neurons were mediated *via* p75, while the effects of GDNF were perhaps mediated indirectly.

IB_4 labels small DRG neurons with mostly unmyelinated axons that are classed as non-peptidergic nociceptive neurons (Hunt and Mantyh, 2001; Fang et al., 2006). They express the GDNF receptor (Molliver et al., 1997; Bennett et al., 1998) and are responsive to GDNF (Bennett et al., 1998; Gavazzi et al., 1999) especially in the presence of laminin (Tucker et al., 2006). It has been reported that IB_4-binding neurons regenerate poorly after PN injury (Leclere et al., 2007), however we found that the proportion of regenerate FG^+ DRG neurons that were immunoreactive for IB_4 was similar (between 30 and 40%) in control and experimental groups. The exception was the NT-3 group, in which there was a significant increase in the proportion of regenerate FG^+ neurons that were $IB_4{}^+$. These sensory neurons may well give rise to many of the unmyelinated axons described in a previous ultrastructural study (Godinho et al., 2013). Conversely, in the acellular and CNTF groups the percentage of $IB_4{}^+$ neurons was lower, a difference that was significant when compared to the NT3 and NGF groups. These new DRG data are entirely consistent with earlier counts of $IB_4{}^+$ axons within engineered grafts, there being significantly more regenerating axons in the NT-3 group (Godinho et al., 2013), but given that the $IB_4{}^+$ sensory population is responsive to GDNF and is distinct from the $TrkC^+$ population of sensory neurons this result is surprising (Gavazzi et al., 1999; Marmigere and Ernfors, 2007). There was a trend for a greater percentage of $IB4^+$ sensory neurons in the GDNF group, but as stated earlier there were significantly fewer FG^+ DRG neurons in the CGRP group overall, thus axon trapping within these grafts may have influenced neuronal counts. Note that, as for p75, $IB_4{}^+$ pericellular ring-like profiles were commonly seen around neurons. After PN injury, these profiles have been reported to be associated with neuronal sprouts and satellite glial cells (Li and Zhou, 2001).

The proportion of regenerate DRG neurons immunoreactive for CGRP or IB_4 was relatively low in animals with grafts containing SCs transduced with CNTF, even though in this group the total number of FG^+ sensory neurons was higher than of any of the other growth factor groups (Fig. 4). Presumably the impact of CNTF was comparatively more marked in the medium-to-large population of sensory neurons (Sango et al., 2008).

4.2. Motor neurons

Longitudinal sections of grafts were stained with an antibody to central ChAT to obtain information about the regenerative growth of motor neurons (Fig. 5). Counts at the proximal, middle and distal ends revealed that the significantly lower numbers of $ChAT^+$ fibers in GDNF and NT-3 grafts appeared in part to be due to a failure to enter from the proximal nerve stump. The number of $ChAT^+$ axons in the NGF group was also relatively low, although not significantly different from other groups. Spinal motor neurons have been shown to express cognate receptors for BDNF, NT-3 and GDNF (Merlio et al., 1992; Henderson et al., 1993; Soler et al., 1999; Richner et al., 2014; Tovar-Y-Romo et al., 2014), and they also express the neurotrophins themselves (Buck et al., 2000). Thus the paucity of $ChAT^+$ profiles in reconstituted nerve grafts containing SCs engineered to express GDNF or NT-3 is unexpected. In comparison, after injections of LV encoding neurotrophin genes *directly* into peripheal nerve segments, Hoyng et al. (2014) reported that the number of $ChAT^+$ axons, albeit of finer caliber than in controls, was 2× and 4× higher in BDNF and GDNF treated grafts respectively compared to control grafts, the fibers spatially segregated from $CGRP^+$ axons. GDNF has well-established pro-survival and pro-regenerative effects on spinal motor neurons (Henderson et al., 1994; Munson and McMahon, 1997; Gould et al., 2008) but the effects are dependent on dose and perhaps also the time that GDNF is made available (Shakhbazau et al., 2013; Marquardt et al., 2015; Eggers et al., 2019; Fadia et al., 2020). In the present study, GDNF release was presumably sustained over 10 weeks, affecting graft morphology and trapping regowing axons within the graft itself, but seemingly also restricting entry into the grafts at its proximal attachment to host peroneal nerve. Note here that the number of $ChAT^+$ axons in BDNF grafts, a neurotrophin shown previously to have dose-dependent effects on motor neuron regrowth (Richner et al., 2014), was similar to the other graft groups, including normal nerves.

In 7 groups, counts of FG^+ motor neurons were made in L4-L6 segments of spinal cord after injection of FG into host peroneal nerve distal to the grafts. Due to processing issues, regions of the lumbar spinal cord from the LV-BDNF and LV-GDNF groups could not be analyzed, however counts of regenerate motor neuron numbers were not significantly different in all other groups (Fig. 8). The FG^+ cell count for the NT-3 group was higher than expected given the relatively low number of $ChAT^+$ axons observed in nerve grafts themselves (see above). A possible reason for this is that NT-3 is an important neurotrophic factor for γ-motor neurons during development (Kucera et al., 1995; Wooley et al., 1999) and their nerve fibers are smaller than those originating from α-motor neurons; such axons may exhibit less ChAT expression and hence may have been more difficult to detect in the immunostained material. Although data on motor neuron numbers were not available in GDNF treated animals, as stated above the number of cholinergic motor fibers was also significantly lower in this group, which may be associated with axon trapping but, similar to NT-3, may also reflect that GDNF has growth promoting effects on the smaller γ-motor neurons (Gould et al., 2008).

It has previously been reported that NeuN does not stain γ-motor neurons (Mullen et al., 1992; Friese et al., 2009). These neurons, which innervate intrafusal muscle fibers and modulate muscle spindle activity,

are also positive for the transcription factor Err3 (Friese et al., 2009). Consistent with these earlier studies, in each of the 7 analyzed groups there was a proportion of FG^+ motor neurons that did not possess detectable NeuN immunoreactivity. The normal distribution of smaller γ-motor neurons to the larger α-motor neurons in rat lumbar ventral horn has been estimated to be about 30:70 (Hashizume et al., 1988; Roy et al., 2007; Friese et al., 2009). In our study, about 40% of FG^+ cells in normal rats were not immunoreactive for NeuN. This ratio was similar in all graft groups but there was a trend for a higher proportion in CNTF treated grafts and especially in NT-3 grafts where the proportion of NeuN negative FG^+ motor neurons was 82%, significantly higher than the group containing SCs transduced only with GFP. Overall, compared to uninjured control, regenerate FG^+ motor neurons were slightly smaller (Fig. 8B), and it is of note that neuronal size in the NT-3 group was not significantly different from other graft groups even though the majority of these labeled cells were NeuN negative γ-motor neurons. Many of these usually small neurons were indeed small to medium-sized, but some were larger in diameter. Some motor neurons may swell after axotomy (McIlwain and Hoke, 2005), and the neurotrophic effects of NT-3 on γ- motor neurons (Kucera et al., 1995; Wooley et al., 1999) may also have resulted in a relative increase in cell body size.

Finally, double immunostaining for the glutamate transporter VGLUT-1 and βIII-tubulin revealed a consistent (about 75–80%) reduction in the number of VGLUT-1 immunoreactive terminals located adjacent to the soma of α-motor neurons in rats with peroneal nerve grafts when compared to uninjured controls. Importantly however, this 'synaptic stripping', assessed 10 weeks post-transplantation, was found to be significant only in the group that received nerve grafts lacking SCs, suggesting that the presence of SCs and expression of relevant neurotrophic factors can partially restore connectivity. Excitatory VGLUT-1 synapses on α-motor neurons (Friese et al., 2009) are associated with input from 1a proprioceptive afferent fibers (Oliveira et al., 2003; Liu et al., 2014; Zhu et al., 2016). While most appear to have remained permanently withdrawn in the grafted animals (see also Alvarez et al., 2011), occasional VGLUT-1 positive terminals were seen in close contact with regenerate FG^+ motor neurons, with a trend for more contacts in grafts with neurotrophin expressing SCs, consistent with an earlier electrophysiological PN injury study in the cat (Mendell et al., 1999) which reported re-establishment of a monosynaptic reflex, particularly with NT-3 treatment.

In conclusion, both GDNF (Whitehead et al., 2005) and NT-3 (Copray and Brouwer, 1994) have been reported to be expressed in intrafusal fibers and muscle spindles, and both factors can support γ-motor neurons. In addition, proprioceptive sensory neurons express TrkC (Marmigere and Ernfors, 2007), the cognate receptor for NT-3, the neurotrophin known to play an essential role in the formation of monosynaptic sensory-motor circuits in ventral spinal cord (Imai and Yoshida, 2018). In our peroneal repair model, grafts containing SCs expressing NT-3 displayed unique characteristics; more IB_4^+ and $CGRP^+$ neurons and axons (Godinho et al., 2013) were seen in NT-3 treated grafts, fewer $ChAT^+$ axons overall, but there was a greater proportion of regenerating γ- motor neurons and seemingly more proprioceptive VGLUT-1 contacts on α-motor neurons. While, in another graft model involving direct LV injection into sciatic autografts, BDNF and GDNF were reported to impair motor recovery and NGF impair sensory recovery (Hoyng et al., 2014), in our graft model using genetically engineered chimeric PN grafts functional locomotor changes were most evident in the NT-3 group (Godinho et al., 2013). Although locomotor behaviour can be influenced by neurotrophin-induced sensory neuropathy and hypersensitivity (Anand, 2004), it is tempting to speculate that in NT-3 grafts in particular there was at least partial restoration of functionally relevant monosynaptic proprioceptive sensory-motor relays *via* the regenerate peroneal nerve, similar to that described after chronic NT-3 infusion in the cat (Mendell et al., 1999). Interestingly, this same neurotrophin delivered into peripheral nerve *via* adeno-associated viral vectors reduces degenerative dendritic changes in motor neurons after lumbar spinal cord injury, and stimulates functionally effective reorganization of descending propriospinal circuitry (Han et al., 2019). Taken together, and noting promising data from primate studies (Fadia et al., 2020), the use of bridging substrates that deliver appropriate neurotrophic factors, or a combinations of such factors, may soon be a more routine approach to the clinical repair of large peripheral nerve defects.

Author contributions

All authors assisted in manuscript preparation and editing. MJG was involved in experimental design, prepared transfected Schwann cells and nerve grafts, carried out FluoroGold injections, perfused and prepared all tissues for histology, cut and analyzed DRG material; JLS cut, immunostained and analyzed all spinal cord material, and prepared most figures; VSK prepared and analyzed immunstained ChAT material in nerve grafts; SIH assisted in analysis of all data and in figure preparation; MAP prepared Schwann cell cultures and transfection with LV, and assisted in reconstitution of nerve grafts; DG analyzed DRG material; LT carried out nerve graft microsurgery; JV and GWP assisted in experimental design and analysis, JV provided lentiviral vector constructs; ARH was involved in experimental design, supervision, analysis of all material, and prepared initial and final manuscript drafts.

Acknowledgements

The work and MJG were supported in the early stages by funds from the Princess Margaret Hospital for Children, Subiaco, Australia. MJG was supported by an Australian Postgraduate Award from The University of Western Australia and by a Mary and Elsie Stevens Bursary from the Australian Federation of University Women. The work was also supported by grants from the WA Neurotrauma Research Program.

References

Alvarez, F.J., Titus-Mitchell, H.E., Bullinger, K.L., Krazpulski, M., Nardelli, P., Cope, T.C., 2011. Permanent central disconnection of proprioceptors after nerve injury and regeneration. I. Loss of VGLUT/1A synapses on motoneurons. J. Neurophysiol. 106, 2450–2470.

Anand, P., 2004. Neurotrophic factors and their receptors in human sensory neuropathies. Prog. Brain Res. 146, 477–492.

Atherton, D.D., Taherzadeh, O., Facer, P., Elliot, D., Anand, P., 2006. The potential role of nerve growth factor (NGF) in painful neuromas and the mechanism of pain relief by their relocation to muscle. J. Hand Surg. 31, 652–656.

Averill, S., McMahon, S.B., Clary, D., Reichardt, L.F., Priestley, J.V., 1995. Immunocytochemical localization of trkA receptors in chemically identified subgroups of adult rat sensory neurons. Eur. J. Neurosci. 7, 1484–1494.

Bennett, D.L., Dmietrieva, N., Priestley, J.V., Clary, D., McMahon, S.B., 1996. trkA, CGRP and IB4 expression in retrogradely labeled cutaneous and visceral primary sensory neurones in the rat. Neurosci. Lett. 206, 33–36.

Bennett, D.L., Michael, G.J., Ramachandran, N., Munson, J.B., Averill, S., Yan, Q., McMahon, S.B., Priestley, J.V., 1998. A distinct subgroup of small DRG cells express GDNF receptor components and GDNF is protective for these neurons after nerve injury. J. Neurosci. 18, 3059–3072.

Buck, C.R., Seburn, K.L., Cope, T.C., 2000. Neurotrophin expression by spinal motoneurons in adult and developing rats. J. Comp. Neurol. 416, 309–318.

Copray, J.C.V.M., Brouwer, N., 1994. Selective expression of neurotrophin-3 messenger RNA in muscle spindles of the rat. Neuroscience 63, 1125–1135.

Cui, Q., Pollett, M.A., Symons, N.A., Plant, G.W., Harvey, A.R., 2003. A new approach to CNS repair using chimeric peripheral nerve grafts. J. Neurotrauma 20, 17–31.

Eggers, R., Hendriks, W.T.J., Tannemaat, M.R., Heerikhuize, J.J.V., Pool, C.W., Carlstedt, T.P., Zaldumbide, A., Hoeben, R.C., Boer, G.J., Verhaagen, J., 2008. Neuroregenerative effects of lentiviral vector-mediated GDNF expression in re-implanted ventral roots. Mol. Cell. Neurosci. 39, 105–117.

Eggers, R., Tannemaat, M.R., Ehlert, E.M., Verhaagen, J., 2010. A spatio-temporal analysis of motoneuron survival, axonal regeneration and neurotrophic factor expression after lumbar ventral root avulsion and implantation. Exp. Neurol. 223, 207–220.

Eggers, R., de Winter, F., Hoyng, S.A., Hoeben, R.C., Malessy, M.J.A., Tannemaat, M.R., Verhaagen, J., 2019. Timed GDNF gene therapy using an immune-evasive gene switch promotes long distance axon regeneration. Brain 142, 295–311.

Fadia, N.B., Bliley, J.M., DiBernardo, G.A., Crammond, D.J., Schilling, B.K., Sivak, W.N., Spiess, A.M., Washington, K.M., Waldner, M., Liao, H.T., James, I.B., Minteer, D.M., Tompkins-Rhoades, C., Cottrill, A.R., Kim, D.Y., Schweizer, R., Bourne, D.A., Panagis, G.E., Asher Schusterman 2nd, M., Egro, F.M., Campwala, I.K., Simpson, T., Weber,

D.J., Gause 2nd, T., Brooker, J.E., Josyula, T., Guevara, A.A., Repko, A.J., Mahoney, C.M., Marra, K.G., 2020. Long-gap peripheral nerve repair through sustained release of a neurotrophic factor in nonhuman primates. Sci. Transl. Med. 12, 527.
Fang, X., Djouhri, L., McMullen, S., Berry, C., Waxman, S.G., Okuse, K., Lawson, S.N., 2006. Intense isolectin-B4 binding in rat dorsal root ganglion neurons distinguishes C-fiber nociceptors with broad action potentials and high Nav1.9 expression. J. Neurosci. 26, 7281–7292.
Friese, A., Kaltschmidt, J.A., Ladle, D.R., Sigrist, M., Jessell, T.M., Arber, S., 2009. Gamma and alpha motor neurons distinguished by expression of transcription factor Err3. Proc. Natl. Acad. Sci. 106, 13588–13593.
Gavazzi, I., Kumar, R.D.C., McMahon, S.B., Cohen, J., 1999. Growth responses of different subpopulations of adult sensory neurons to neurotrophic factors in vitro. Eur. J. Neurosci. 11, 3405–3414.
Godinho, M.J., Teh, L., Pollett, M.A., Goodman, D., Hodgetts, S.I., Sweetman, I., Walters, M., Verhaagen, J., Plant, G.W., Harvey, A.R., 2013. Immunohistochemical, ultrastructural and functional analysis of axonal regeneration through peripheral nerve grafts containing Schwann cells expressing BDNF, CNTF or NT3. PLoS One 8 (8), e69987.
Gordon, T., 2009. The role of neurotrophic factors in nerve regeneration. Neurosurg. Focus. 26, 1–10.
Gould, T.W., Yonemura, S., Oppenheim, R.W., Ohmori, S., Enomoto, H., 2008. The neurotrophic effects of glial cell line-derived neurotrophic factor on spinal motoneurons are restricted to fusimotor subtypes. J. Neurosci. 28, 2131–2146.
Gulati, A.K., 1995. Immunological fate of Schwann cell-populated acelluar basal lamina nerve grafts. Transplantation 59, 1618–1622.
Hammarberg, H., Piehl, F., Cullheim, S., Fjell, J., Hökfelt, T., Fried, K., 1996. GDNF mRNA in Schwann cells and DRG satellite cells after chronic sciatic nerve injury. NeuroReport 22, 857–860.
Han, Q., Ordaz, J.D., Liu, N.K., Richardson, Z., Wu, W., Xia, Y., Qu, W., Wang, Y., Dai, H., Zhang, Y.P., Shields, C.B., Smith, G.M., Xu, X.M., 2019. Descending motor circuitry required for NT-3 mediated locomotor recovery after spinal cord injury in mice. Nat. Commun. 10, 5815.
Harpf, C., Dabernig, J., Humpel, C., 2002. Receptors for NGF and GDNF are highly expressed in human peripheral nerve neuroma. Muscle Nerve 25, 612–615.
Hashizume, K., Kanda, K., Burke, R.E., 1988. Medial gastrocnemius motor nucleus in the rat: age-related changes in the number and size of motoneurons. J. Comp. Neurol. 269, 425–430.
Henderson, C.E., Camu, W., Clement, M., Gouin, A., Poulsen, K., Karihaloo, M., Rullomas, M., Evans, T., McMahon, S.B., Armanini, M., Berkemeier, L., Phillips, H., Rosenthal, A., 1993. Neurotrophins promote motor neuron survival and are present in embryonic limb bud. Nature 363, 266–270.
Henderson, C.E., Phillips, H.S., Pollock, R.A., Davies, A.M., Lemeulle, C., Armanini, M., Simmons, L., Moffet, B., Vandlen, R.A., Simmons, L., Koliatsos, V.E., Rosenthal, A., 1994. GDNF: a potent survival factor for motoneurons present in peripheral nerve and muscle. Science 266, 1062–1064.
Hoyng, S.A., De Winter, F., Gnavi, S., de Boer, R., Boon, L.I., Korvers, L.M., Tannemaat, M.R., Malessy, M.J., Verhaagen, J., 2014. A comparative morphological, electrophysiological and functional analysis of axon regeneration through peripheral nerve autografts genetically modified to overexpress BDNF, CNTF, GDNF, NGF, NT3 or VEGF. Exp. Neurol. 216, 578–593.
Hu, Y., Leaver, S.G., Plant, G.W., Hendricks, W.T.J., Niclou, S.P., Verhaagen, J., Harvey, A.R., Cui, Q., 2005. Lentiviral-mediated transfer of CNTF to Schwann cells within reconstructed peripheral nerve grafts enhances adult retinal ganglion cell survival and axonal regeneration. Mol. Ther. 11, 906–915.
Hu, Y., Arulpragasam, A., Plant, G.W., Hendriks, W.T.J., Cui, Q., Harvey, A.R., 2007. The importance of transgene and cell type on the regeneration of adult retinal ganglion cell axons within reconstituted bridging grafts. Exp. Neurol. 207, 314–328.
Hunt, S.P., Mantyh, P.W., 2001. The molecular dynamics of pain control. Nat. Rev. Neurosci. 2, 83–91.
Imai, F., Yoshida, Y., 2018. Molecular mechanisms underlying monosynapic sensory-motor circuit development in the spinal cord. Dev. Dyn. 247, 581–587.
Ip, N.Y., McClain, J., Barrezueta, N.X., Aldrich, T.H., Pan, L., Li, Y., Wiegand, S.J., Friedman, B., Davis, S., Yancapoulos, G.D., 1993. The α component of the CNTF receptor is required for signaling and defines potential CNTF targets in the adult during development. Neuron 10, 89–102.
Ju, G., Hökfelt, T., Brodin, E., Fahrenkrug, J., Fischer, J.A., Frey, P., Elder, R.P., Brown, J.C., 1987. Primary sensory neurons of the rat showing calcitonin gene-related peptide immunoreactivity and their relation to substance P-, somatostatin-, galanin-, vasoactive intestinal polypeptide- and cholecystokinin-immunoreactive ganglion cells. Cell Tissue Res. 247, 417–431.
Kalous, A., Keast, J.R., 2010. Conditioning lesions enhance growth state only in sensory neurons lacking calcitonin gene-related peptide and isolectin B4-biding. Neuroscience 166, 107–121.
Krishnan, V.S., White, Z., McMahon, C., Hodgetts, S.I., Fitzgerald, M., Shavlakadze, T., Harvey, A.R., Grounds, M.D., 2016. A neurogenic perspective of sarcopenia: time course study of sciatic nerves from aging mice. J. Neuropathol. Exp. Neurol. 75, 464–478.
Krishnan, V.S., Shavlakadze, T., Grounds, M.D., Hodgetts, S.I., Harvey, A.R., 2018. Age-related loss of VGLUT1 excitatory, but not VGAT inhibitory, contacts on motor neurons in spinal cords of old male mice. Biogerontology 19, 385–399.
Kucera, J., Ernfors, P., Walro, J., Jaenisch, R., 1995. Reduction in the number of spinal motor neurons in neurotrophin-3-deficient mice. Neuroscience 69, 321–330.
Leclere, P.G., Norman, E., Groutsi, F., Coffin, R., Mayer, U., Pizzey, J., Tonge, D., 2007. Impaired axonal regeneration by isolectin B4-binding dorsal root ganglion neurons in vitro. J. Neurosci. 27, 1190–1199.
Lee, N., Spearry, R.P., Leahy, K.M., Robitz, R., Trinh, D.S., Mason, C.O., Zurbrugg, R.J., Batt, M.K., Paukl, R.J., Maclennan, A.J., 2013. Muscle ciliary neurotrophic factor receptor α promotes axonal regeneration and functional recovery following peripheral nerve lesion. J. Comp. Neurol. 521, 2947–2965.
Lee, N., Spearry, R.P., Rydyznski, C.E., Maclennan, A.J., 2019. Muscle ciliary neurotophic factor receptor α contributes to motor neuron STAT3 activation following peripheral nerve lesion. Eur. J. Neurosci. 49, 1084–1090.
Levine, A.J., Hinckley, C.A., Hilde, K.L., Driscoll, S.P., Poon, T.H., Montgomery, J.M., Pfaff, S.L., 2014. Identification of a cellular node for motor control pathways. Nat. Neurosci. 17, 586–593.
Li, L., Zhou, X.F., 2001. Pericellular Griffonia simplicifolia 1 isolectin B4-binding ring structures in the dorsal root ganglia following peripheral nerve injury in rats. J. Comp. Neurol. 439, 259–274.
Liu, C., Ward, P.J., English, A.W., 2014. The effects of exercise on synaptic stripping require androgen receptor signaling. PLoS One 9 e98633.
Lo, A.C., Li, L., Oppenheim, R.W., Prevette, D., Houenou, L.J., 1995. Ciliary neurotrophic factor promotes the survival of spinal sensory neurons following axotomy but not during the period of programmed cell death. Exp. Neurol. 134, 49–55.
MacLennan, A.J., Vinson, E.N., Marks, L., McLaurin, D.L., Pfeifer, M., Lee, N., 1996. Immunohistochemical localization of ciliary neurotrophic factor receptor α receptor expression in the rat nervous system. J. Neurosci. 16, 621–630.
MacLennan, A.J., Devlin, B.K., Neitzel, K.L., McLaurin, D.L., Anderson, K.J., Lee, N., 1999. Regulation of ciliary neurotrophic factor receptor alpha in sciatic motor neurons following axotomy. Neuroscience 91, 1401–1413.
Marmigere, F., Ernfors, P., 2007. Specification and connectivity of neuronal subtypes in the sensory lineage. Nat. Rev. Neurosci. 8, 114–127.
Marquardt, L.M., Ee, X., Nisha Iyer, M.S., Hunter, D., Mackinnon, S.E., Wood, M.E., Sakiyama-Elbert, S.E., 2015. Finely tuned temporal and spatial delivery of GDNF promotes enhanced nerve regeneration in a long nerve defect model. Tissue Eng. A 21, 2852–2864.
McIlwain, D.L., Hoke, V.B., 2005. The role of the cytoskeleton in cell body enlargement, increased nuclear eccentricity and chromatolysis in axotomized spinal motor neurons. BMC Neurosci. 6, 19.
Mendell, L.M., Johnson, R.D., Munson, J.B., 1999. Neurotrophin modulation of the monosynaptic reflex after peripheral nerve transection. J. Neurosci. 19, 3162–3170.
Merlio, J.P., Ernfors, P., Jaber, M., Persson, H., 1992. Molecular cloning of rat trkC and distribution of cells expressing messenger RNAs for members of the trk family in the rat central nervous system. Neuroscience 51, 513–532.
Michael, G.J., Averill, S., Nitkunan, A., Rattray, M., Bennett, D.L., Yan, Q., Priestley, J.V., 1997. Nerve growth factor treatment increases brain-derived neurotrophic factor selectively in TrkA-expressing dorsal root ganglion cells and in their central terminations within the spinal cord. J Neurosci. 17, 8476–8490`.
Molliver, D.C., Wright, D.E., Leitner, M.L., Parsadanian, A.S., Doster, K., Wen, D., Yan, Q., Snider, W.D., 1997. IB_4-binding DRG neurons switch from NGF to GDNF dependence in early postnatal life. Neuron 19, 849–861.
Morrissey, T.K., Kleitman, N., Bunge, R.P., 1991. Isolation and functional characterization of Schwann cells derived from adult peripheral nerve. J. Neurosci. 11, 2433–2442.
Mullen, R.J., Buck, C.R., Smith, A.M., 1992. NeuN, a neuronal specific nuclear protein in vertebrates. Development 116, 201–211.
Munson, J.B., McMahon, S.B., 1997. Effects of GDNF on axotomised sensory and motor neurons in adult rats. Eur. J. Neurosci. 9, 1126–1129.
Oliveira, A.L., Hydling, F., Olsson, E., Shi, T., Edwards, R.H., Fujiyama, F., Kaneko, T., Hökfelt, T., Cullheim, S., Meister, B., 2003. Cellular localization of three vesicular glutamate transporter mRNAs and proteins in rat spinal cord and dorsal root ganglia. Synapse 50, 117–129.
Plant, G.W., Currier, P.F., Cuervo, E.P., Bates, M.L., Pressman, Y., Bunge, M.B., Wood, P.M., 2002. Purified adult ensheathing glia fail to myelinate axons under culture conditions that enable Schwann cells to form myelin. J. Neurosci. 22, 6083–6091.
Richner, M., Ulrichsen, M., Elmegaard, S., Dieu, R., Pallesen, L.T., Vaegter, C.B., 2014. Peripheral nerve injury modulates neurotrophin signaling in the peripheral and central nervous system. Mol. Neurobiol. 50, 945–970.
Roy, R.R., Matsumoto, A., Zhong, H., Ishihara, A., Edgerton, V.R., 2007. Rat alpha- and gamma-motoneuron soma size and succinate dehydrogenase activity are independent of neuromuscular activity level. Muscle Nerve 36, 234–241.
Sango, K., Yanagisawa, H., Komuta, Y., Si, Y., Kawano, H., 2008. Neuroprotective properties of ciliary neurotrophic factor for cultured adult rat dorsal root ganglion neurons. Histochem. Cell Biol. 130, 669–679.
Santosa, K.B., Jesuraj, N.J., Viader, A., MacEwan, M., Newton, P., Hunter, D.A., Mackinnon, S.E., Johnson, P.J., 2013. Nerve allografts supplemented with Schwann cells overexpressing glial cell line-derived neurotrophic factor. Muscle Nerve 47, 213–223.
Shakhbazau, A., Kawasoe, J., Hoyng, S.A., Kumar, R., van Minnen, J., Verhaagen, J., Midha, R., 2012. Early regenerative effects of NGF-transduced Schwann cells in peripheral nerve repair. Mol. Cell. Neurosci. 50, 103–112.
Shakhbazau, A., Mohanty, C., Shcharbin, D., Bryszewska, M., Caminade, A.M., Majoral, J.P., Alant, J., Midha, R., 2013. Doxycycline-regulated GDNF expression promotes axonal regeneration and functional recovery in transected peripheral nerve. J. Control. Release 172, 841–851.
Soler, R.M., Dolcet, X., Encinas, M., Egea, J., Bayascas, J.R., Comella, J.X., 1999. Receptors of the glial cell line-derived neurotrophic factor family of neurotrophic factors signal cell survival through phosphatidylinositol 3-kinase pathways in spinal motor neurons. J. Neurosci. 19, 9160–9169.
Stucky, C.L., Koltzenburg, M., 1997. The low-affinity neurotrophin receptor p75 regulates the function but not the selective survival of specific subpopulations of sensory neurons. J. Neurosci. 17, 4398–4405.
Stucky, C.L., Lewin, G.R., 1999. Isolectin B4-positive and -negative nociceptors are functionally distinct. J. Neurosci. 19, 6497–6505.

Swett, J.E., Torigoe, Y., Elie, V.R., Bourassa, C.M., Miller, P.G., 1991. Sensory neurons of the rat sciatic nerve. Exp. Neurol. 114, 82–103.
Symons, N.A., Danielsen, N., Harvey, A.R., 2001. Migration of cells into and out of peripheral nerve isografts in the peripheral and central nervous systems of the adult mouse. Eur. J. Neurosci. 14, 522–532.
Tannemaat, M.R., Eggers, R., Hendriks, W.T., Ruiter, G.C.W.D., Heerikhuize, J.J.V., Pool, C.W., Malessy, M.J., Boer, G.J., Verhaagen, J., 2008. Differential effects of lentiviral vector-mediated overexpression of nerve growth factor and glial cell line-derived neurotrophic factor on regenerating sensory and motor axons in the transected peripheral nerve. Eur. J. Neurosci. 28, 1467–1479.
Todd, A.J., Hughes, D.I., Polgar, E., Nagy, G.G., Mackie, M., Ottersen, O.P., Maxwell, D.J., 2003. The expression of vesicular glutamate transporters VGLUT1 and VGLUT2 in neurochemically defined axonal populations in the rat spinal cord with emphasis on the dorsal horn. Eur. J. Neurosci. 17, 13–27.
Tovar-Y-Romo, L.B., Ramírez-Jarquín, U.N., Lazo-Gómez, R., Tapia, R., 2014. Trophic factors as modulators of motor neuron physiology and survival: implications for ALS therapy. Front. Cell. Neurosci. 8, 61.
Tucker, B.A., Rahimtula, M., Mearow, K.M., 2006. Laminin and growth factor receptor activation stimulates differential growth responses in subpopulations of adult DRG neurons. Eur. J. Neurosci. 24, 676–690.
Whitehead, J., Keller-Peck, C., Kucera, J., Tourtellotte, W.G., 2005. Glial cell-line derived neurotrophic factor-dependent fusimotor neuron survival during development. Mech. Dev. 122, 27–41.
Wooley, A., Sheard, P., Dodds, K., Duxson, M., 1999. Alpha motoneurons are present in normal numbers but with reduced soma size in neurotrophin-3 knockout mice. Neurosci. Lett. 272, 107–110.
Wright, D.E., Snider, W.D., 1995. Neurotrophin receptor mRNA expression defines distinct populations of neurons in rat dorsal root ganglia. J. Comp. Neurol. 351, 329–338.
Zhou, X.-F., Rush, R.A., McLachlan, E.M., 1996. Differential expression of the p75 nerve growth factor receptor in glia and neurons of the rat dorsal root ganglia after peripheral nerve transection. J. Neurosci. 19, 2901–2911.
Zhou, X.-F., Deng, Y.-S., Chie, E., Xue, Q., Zhong, J.-H., McLachlan, E.M., Rush, R.A., Xian, C.J., 1999. Satellite-cell-derived nerve growth factor and neurotrophin-3 are involved in noradrenergic sprouting in the dorsal root ganglia following peripheral nerve injury in the rat. Eur. J. Neurosci. 11, 1711–1722.
Zhu, X., Ward, P.J., English, A.W., 2016. Selective requirement for maintenance of synaptic contacts onto motoneurons by target-derived trkB receptors. Neural Plast 2016 e2371893.